Electronic Supplementary Information (ESI)

A BODIPY-based fluorescent sensor for the detection of Pt^{2+} and Pt drugs

Fung-Kit Tang,[a] Jiaqian Zhu,[b] Fred Ka-Wai Kong,[c] Maggie Ng,[c] Qingyuan Bian,[a] Vivian Wing-Wah Yam,*[c] Anfernee Kai-Wing Tse,*[d] Yu-Chung Tse*[e] and Ken Cham-Fai Leung*[a]

[a] Department of Chemistry, State Key Laboratory of Environmental and Biological Analysis, Hong Kong Baptist University, Kowloon Tong, Kowloon, Hong Kong SAR, P. R. China

[b] Centre for Cancer and Inflammation Research, School of Chinese Medicine, Hong Kong Baptist University, Kowloon Tong, Kowloon, Hong Kong SAR, P. R. China

[c] Department of Chemistry, The University of Hong Kong, Pokfulam Road, Hong Kong SAR, P. R. China

[d] Programme of Food Science and Technology, Division of Science and Technology, Beijing Normal University-Hong Kong Baptist University United International College, Zhuhai 519087, P. R. China

[e] Guangdong Provincial Key Laboratory of Cell Microenvironment and Disease Research, Department of Biology, Southern University of Science and Technology (SUSTech), Shenzhen, 518055, P. R. China

*E-mail: cfleung@hkbu.edu.hk, wwyam@hku.hk, kaiwingtse@uic.edu.hk, tseyc@sustech.edu.cn

Table of Contents

General information for experiments

General synthetic materials and methods:

Chemicals or reagents were purchased from Sigma Aldrich., Acros, Dieckmann, J&K, Alfa Aesar or TCI, and used as received. All solvents were used directly without further treatment or distillation. Silica gel 60 (70–230 mesh, Merck) was used for column chromatography. Thin Layer Chromatography (TLC) was performed using F_{254} silica (aluminum sheet back plates, Merck).

Instruments and spectroscopic methods:

NMR spectroscopy

NMR spectra were recorded from Bruker Advance–III 400 NMR spectrometer operating at 400 MHz for ^{1}H and 101 MHz for $^{13}C\{^{1}H\}$, respectively. Chemical shifts are quoted in ppm. ^{1}H and ^{13}C chemical shifts were referenced internally with solvent residue chemical shift values ($CDCl_3$: ^{1}H, 7.26 ppm; ^{13}C, 77.16 ppm; CD_3OD: ^{1}H, 3.31 ppm; ^{13}C, 49.00 ppm; $(CD_3)_2CO$: ^{1}H, 29.84 ppm; ^{13}C, 206.26 ppm). ^{195}Pt NMR spectra were recorded on a Bruker Ascend™ 500 Fourier–transform NMR spectrometer with chemical shifts reported relative to K_2PtCl_4 in D_2O ($\delta = -1617$ ppm). NMR data were processed using MestReNova Software (Mestrelab).

Mass Spectrometry

High-resolution mass spectra were recorded on a Bruker Autoflex mass spectrometer (MALDI–TOF) and a Thermo Fisher Scientific UPLC–Q exactive focus hybrid quadrupole-orbitrap mass spectrometer in positive ion mode (ESI–MS).

Luminescent spectroscopy

Fluorescence spectra and UV–Vis absorption spectra were collected on a PTI QM–4/2005 spectrometer and an Agilent Cary 8454 UV–Vis Diode Array System, respectively. Solution samples were contained in quartz cuvettes with a volume of 1.5 mL, 1 cm of path length and 0.4 cm of slit length. All aqueous solutions were prepared with Milli-Q water (18.2 MΩ cm^{-1}). Briefly, stock DMF solution of **PS** (1 mM) and stock analyte solutions (10 mM) were freshly prepared and added to aqueous solution according to the detection condition to form a final mixture with a volume of 1 mL. The final concentration of **PS** is 5 μM, and the final concentration of analyte is 100 μM (20 mol equiv.). The final reaction mixture was vortexed and incubated at ambient condition for 6 h before emission measurement of cations and platinum salts; while the final reaction mixture was vortexed and incubated at ambient condition for 6–24 h before emission measurement of organoplatinum drugs. Absolute quantum yields were measured on a Hamamatsu C9920-03 Absolute PL Quantum Yield Measurement System.

Biological assays and cell imaging experiments:

Cell Culture

Human A549 (lung) cancer cells were obtained from American Type Culture Collection (ATCC) and cultured in Dulbecco's modification of Eagle medium (DMEM) supplemented with 10 % fetal bovine serum, 100 units/mL penicillin and 100 mg/mL streptomycin. Cells were cultured at 37 ^{o}C in an atmosphere of 5 % CO_2 and 95 % humidity.

Cell proliferation assay

Cell proliferation was assessed by MTT [3-(4,5-dimethylthiazol-2-yl)-2,5-diphenyltetrazolium] bromide assay. Briefly, cells were plated in 96–well plates (5 x10^3 cells/well) and then treated with **PS** for 24 h. Afterward, cells were treated with MTT reagent and the absorbance at 570 nm was measured using a microplate reader. The viability of control (untreated cells) was regarded as 100 %.

Confocal laser scanning microscopy

For cellular imaging experiments, A549 cells were seeded in 4–well cell culture slides (SPL Life Sciences) and allowed to adhere overnight. Afterward, cells were incubated with Pt(II) derivatives for 4 h, followed by addition of **PS** for 30 min at 37 °C. Cells were then washed twice with PBS and fixed with methanol for 15 min at –20 °C. After fixation, cells were washed three times with PBS. Coverslips were mounted (Fluoroshield Mounting Medium with DAPI; Abcam) onto slides and sealed. Cells were imaged with Leica SP8 confocal microscope using DAPI (for nucleus staining: excitation at 405 nm, detection 440–480 nm) and Alexa 488 filters (excitation at 488 nm, detection 495–545 nm). Images were captured and analyzed with LAS AF software (Leica, Germany).

Computational studies:

All the density functional theory (DFT) calculations were carried out with the Gaussian 09 suite of programs.[1] The ground-state geometries of **PS** and **PS+Pt^{2+}** were fully optimized in water by DFT with the hybrid Perdew, Burke, and Ernzerhof (PBE0) functional,[2-4] in conjunction with the conductor-like polarizable continuum model (CPCM).[5, 6] Regarding **PS+Pt^{2+}**, three binding modes, namely, O^S^S^O, O^S^N^O and O^S^N^S, have been considered and the corresponding Pt(II) complexes have been optimized. Vibrational frequencies of all the stationary points have been calculated to verify that each is a minimum (NIMAG = 0) on the potential energy surface (PES). The Cartesian coordinates of the optimized ground-state geometries of **PS** and **PS+Pt^{2+}** in three binding modes are given in Tables S2–5. The Stuttgart effective core potentials (ECPs) and the associated basis set were used to describe Pt [7] with f-type polarization functions (ζ = 0.993),[8] whereas the 6-31G(d,p) basis set[9-11] was applied for all other atoms. A pruned (99,590) grid was used for numerical integration in the DFT calculations.

Synthetic scheme and preparation of compounds

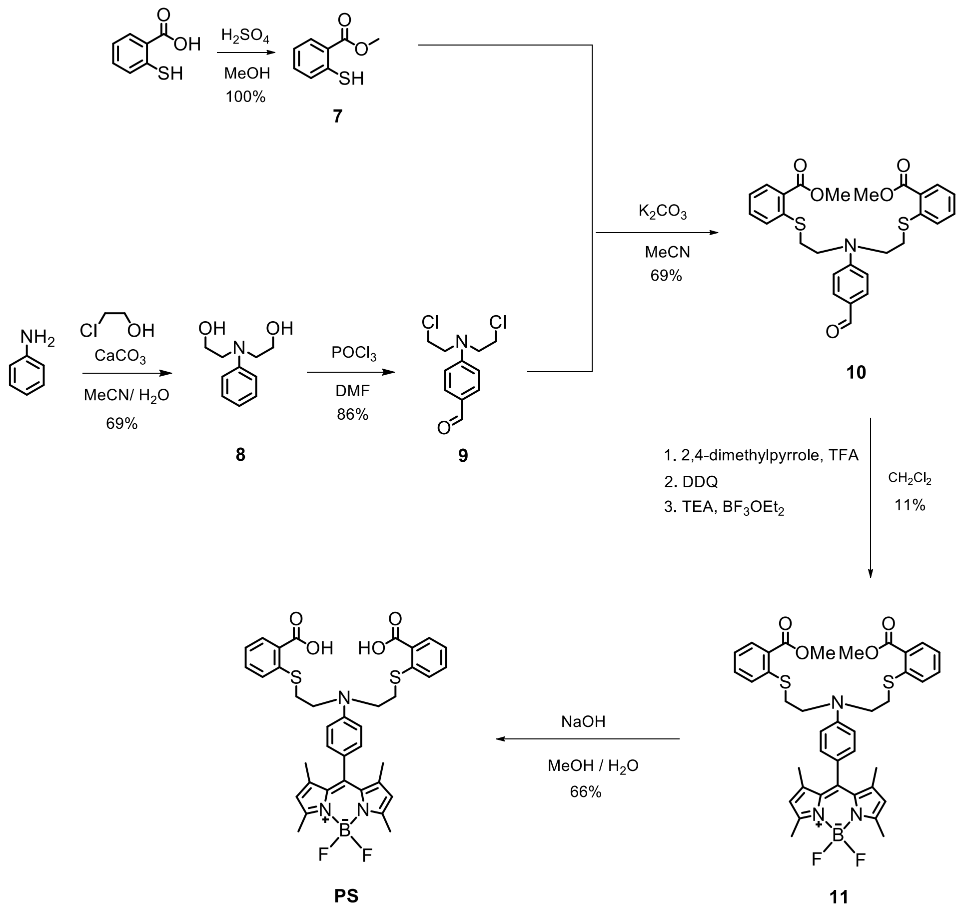

Scheme S1. Synthesis of compounds and chemosensor **PS**.

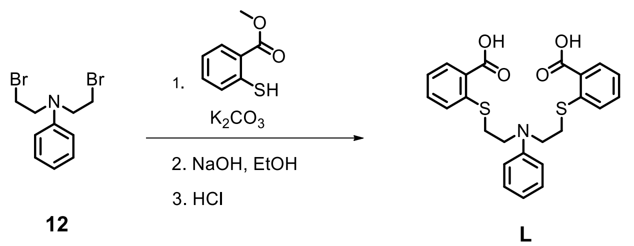

Scheme S2. Synthesis of compound **L**.

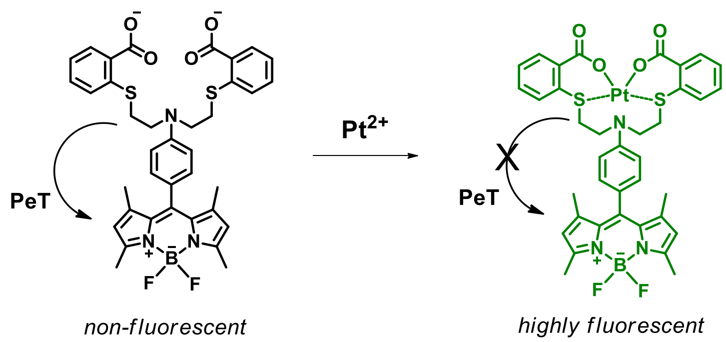

Scheme S3. Proposed detection mechanism of **PS** towards Pt^{2+}.

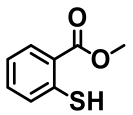

Synthesis of compound **7**

Compound **7** was synthesized with a modified method from the literature.[12] Thiosalicylic acid (4 g, 26 mmol) was dissolved in 40 mL of MeOH, followed by 2 mL of concentrated H_2SO_4 was added, and the mixture was heated to reflux overnight. The mixture was diluted with ice and the diluted solution was neutralized by K_2CO_3. The product was extracted with CH_2Cl_2 (100 mL x 3), the organic layer was washed with brine and dried with anhydrous $MgSO_4$. Solvent was removed to yield a yellow liquid. Yield = 3.7 g, 85 %. ^{1}H NMR (400 MHz, $CDCl_3$, 298 K) δ 8.01 (d, J = 8.0 Hz, 1H), 7.33 – 7.30 (m, 2H), 7.16 (ddd, J = 7.9, 5.3, 3.2 Hz, 1H), 4.68 (s, 1H), 3.92 (s, 3H). ^{13}C NMR (101 MHz, $CDCl_3$, 298 K) δ 167.30, 138.40, 132.61, 131.82, 131.03, 125.93, 124.79, 52.38.

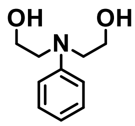

Synthesis of compound **8**

Compound **8** was synthesized with a modified method from the literature.[13] A mixture of aniline (10 g, 107 mmol), chloroethanol (40 g, 497 mmol), $CaCO_3$ (47 g, 470 mmol) and KI (2.7 g, 16.3 mmol) in 120 mL of H_2O/MeCN (v/v = 1:1) solution was refluxed for 4 d. Then insoluble materials were filtered and the filtrate was collected. The filtrate was diluted with 100 mL of H_2O and the product was extracted with CH_2Cl_2 (100 mL x3). The organic layer was concentrated and purified by silica column using CH_2Cl_2/MeOH (*v/v* = 10:1) to give a white solid. Yield = 13.4 g, 69 %. ^{1}H NMR (400 MHz, $CDCl_3$, 298 K, –O*H* proton signal missing) δ 7.23 (dd, *J* = 8.9, 7.2 Hz, 2H), 6.73 (t, *J* = 7.3 Hz, 1H), 6.67 (d, *J* = 8.0 Hz, 2H), 3.80 (t, *J* = 4.8 Hz, 4H), 3.53 (t, *J* = 4.8 Hz, 4H). ^{13}C NMR (101 MHz, $CDCl_3$, 298 K) δ 147.79, 129.39, 116.87, 112.51, 60.83, 55.52.

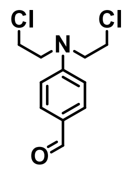

Synthesis of compound **9**

Compound **9** was synthesized with a modified method from the literature.[13] In brief, a 20 mL of $POCl_3$ was added dropwise to 40 mL of DMF solution containing compound **8** (8.65 g, 47.7 mmol) at 0 °C for 2 h. The mixture was warmed to room temperature with stirring overnight. The mixture was diluted with ice water, and the solution was neutralized by K_2CO_3. The product was then extracted with CH_2Cl_2 (100 mL x 2). The organic layer was washed with brine and concentrated by rotary evaporator. The product was purified by silica column using EtOAc/hexane (*v/v* = 1:1) to give a pale yellow solid. Yield = 10.1 g, 86 %. ^{1}H NMR (400 MHz, $CDCl_3$, 298 K) δ 9.78 (s, 1H), 7.77 (d, *J* = 8.9 Hz, 2H), 6.74 (d, *J* = 9.0 Hz, 2H), 3.84 (t, *J* = 6.9 Hz, 4H), 3.68 (t, *J* = 6.8 Hz, 4H). ^{13}C NMR (101 MHz, $CDCl_3$, 298 K) δ 190.32, 151.08, 132.44, 126.86,

111.40, 53.41, 40.15. HRMS (MADLI–TOF): calculated for $C_{11}H_{14}Cl_2NO$ $[M+H]^+$ *m/z* 246.0449, found 246.2818.

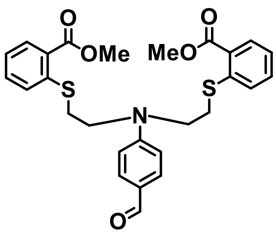

Synthesis of compound **10**

A mixture of compound **7** (1.5 g, 8.9 mmol), K_2CO_3 (3.3 g, 24 mmol) and compound **9** (1 g, 4.1 mmol) in 25 mL of MeCN was refluxed overnight. The insoluble material was filtered and the filtrate was collected. The excess of solvent was removed by rotary evaporator and residue was purified by silica column using EtOAc/hexane (*v/v* = 1:1) to give a yellow liquid. Yield = 1.5 g, 69 %. ^{1}H NMR (400 MHz, $CDCl_3$, 298 K) δ 9.74 (s, 1H), 7.94 (dd, *J* = 7.8, 1.6 Hz, 2H), 7.71 (d, *J* = 8.9 Hz, 2H), 7.40 (ddd, *J* = 8.1, 7.2, 1.6 Hz, 2H), 7.32 (dd, *J* = 8.2, 1.2 Hz, 2H), 7.19 (ddd, *J* = 8.2, 7.3, 1.2 Hz, 2H), 6.67 (d, *J* = 9.0 Hz, 2H), 3.89 (s, 6H), 3.72 (t, *J* = 7.4 Hz, 4H), 3.17 (t, *J* = 7.3 Hz, 4H). ^{13}C NMR (101 MHz, $CDCl_3$, 298 K) δ 189.98, 166.61, 151.09, 139.50, 132.31, 132.11, 131.25, 128.42, 126.08, 125.91, 124.54, 111.10, 52.09, 50.15, 29.26. HRMS (MALDI–TOF): calculated for $C_{27}H_{27}NO_5S_2Na$ $[M+Na]^+$ *m/z* 532.1223, found 532.1217.

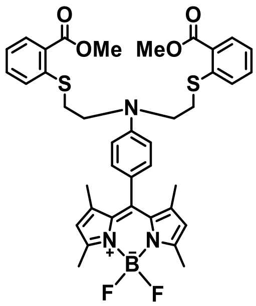

Synthesis of compound **11**

Compound **11** (1.6 g, 3.1 mmol) and 2,4-dimethylpyrrole (0.6 g, 6.3 mmol) were dissolved in 400 mL of degassed CH_2Cl_2, followed by addition of 10 drops of trifluoroacetic acid with stirring at room temperature for 24 h. Then DDQ (0.8 g, 3.5 mmol) was added to the mixture and allowed to react for 4 h at room temperature. 6 mL of triethylamine was added to the mixture, followed by 6 mL of $BF_3{\cdot}OEt_2$ with further stirring for 24 h at room temperature. The organic layer was washed with H_2O (300 mL x 3). The organic layer was concentrated by rotary evaporator and the product was purified by silica gel column chromatography using EtOAc/hexane (*v/v* = 1:1) to afford **11** as orange liquid. Yield = 0.26 g, 11 %. ^{1}H NMR (400 MHz, $CDCl_3$, 298 K) δ 7.96 (dd, *J* = 7.9, 1.5 Hz, 2H), 7.41 (ddd, *J* = 8.1, 7.2, 1.6 Hz, 2H), 7.33 (dd, *J* = 7.9, 0.9 Hz, 2H), 7.20 (ddd, *J* = 7.7, 7.2, 1.2 Hz, 2H), 7.07 (d, *J* = 8.7 Hz, 2H), 6.74 (d, *J* = 8.8 Hz, 2H), 5.97 (s, 2H), 3.91 (s, 6H), 3.71 (t, *J* = 7.4 Hz, 4H), 3.18 (t, *J* = 7.3 Hz, 4H), 2.54 (s, 6H), 1.48 (s, 6H). ^{13}C NMR (101 MHz, $CDCl_3$, 298 K) δ 166.98, 155.06, 147.09, 143.19, 142.63, 140.19, 132.49, 132.19, 131.53, 129.45, 128.67, 126.29, 124.68, 123.30, 121.08, 112.48, 52.34, 50.62, 29.60, 14.90, 14.70. ^{19}F NMR (377 MHz, $CDCl_3$, 298 K) δ -146.17 (q, *J* = 33.0 Hz, 2F). HRMS (MALDI–TOF): calculated for $C_{39}H_{40}BF_2N_3O_4S_2Na$ $[M+Na]^+$ *m/z* 750.2420, found 750.2386.

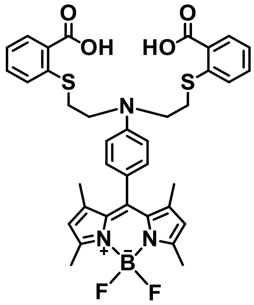

Synthesis of **PS**

Compound **11** (0.26 g, 0.36 mmol) was dissolved in 60 mL of MeOH/H_2O/THF mixture (*v/v/v* = 1:1:1). Then NaOH (0.19 g, 4.75 mmol) was added and the resulting mixture was stirred at room temperature overnight. The excess of solvent was removed by rotary evaporator and the residue was re-dissolved in water with the pH adjusted to around pH 3 by 2 M HCl solution. The precipitate was collected by suction filtration, washed with 50 mL of H_2O and 50 mL of diethyl ether. The product was dried in air to give dark green powder. Yield = 165 mg, 66 %. ^{1}H NMR (400 MHz, CD_3OD, 298 K, –O*H* proton signal missing) δ 11.43 (s, 2H), 7.89 (d, *J* = 7.9 Hz, 2H), 7.53 – 7.31 (m, 4H), 7.27 – 7.07 (m, 4H), 6.87 (d, *J* = 8.1 Hz, 2H), 6.34 (s, 2H), 3.80 (t, *J* = 6.1 Hz, 4H), 3.37 – 3.13 (m, 4H), 2.37 (s, 6H), 1.77 (s, 6H). ^{13}C NMR (101 MHz, $(CD_3)_2CO$, 298 K) δ 167.63, 155.41, 148.52, 144.00, 141.54, 133.26, 132.16, 130.02, 129.61, 127.15, 125.07, 123.23, 121.73, 121.70, 121.53, 113.49, 68.05, 51.11, 26.16, 14.96. ^{19}F NMR (377 MHz, CD_3OD, 298 K) δ -147.02 (q, *J* = 32.4 Hz, 2F). HRMS (+ESI): calculated for $C_{37}H_{37}BF_2N_3O_4S_2$ $[M]^+$ *m/z* 700.2281, found 700.2274.

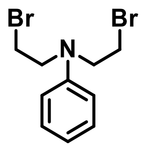

Compound **12**

Compound **12** was prepared according to the literature.[14]

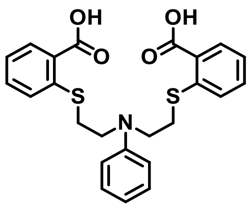

Synthesis of compound **L**

Compound **7** (3.89 g, 23.1 mmol), K_2CO_3 (15 g, 0.11 mol) and compound **12** (3.2 g, 10.4 mmol) in 150 mL of MeCN was refluxed overnight. Insoluble materials were filtered and the filtrate was collected. The filtrate was concentrated and purified by flash column chromatography using EtOAc/hexane (*v/v* = 1:1) to afford a yellow liquid. The yellow liquid was used directly by dissolving in 200 mL of EtOH with NaOH (10 g, 0.25 mol). The mixture was refluxed overnight and then acidified with concentrated HCl to give pale yellow precipitate. The precipitate was collected by suction filtration, washed with water and dried under vacuum to give a solid. The solid product was further recrystallized in EtOH to afford a pale yellow powder. Yield = 4.1 g, 87 %. ^{1}H NMR (400 MHz, CD_3OD, 298 K) δ 7.95 (dd, J = 7.8, 1.6 Hz, 2H), 7.69 – 7.62 (m, 4H), 7.63 – 7.54 (m, 1H), 7.49 (d, J = 7.8 Hz, 2H), 7.35 (d, J = 7.9 Hz, 2H), 7.30 (t, J = 7.5 Hz, 2H), 3.83 (d, J = 8.1 Hz, 4H), 3.07 (d, J = 8.1 Hz, 4H). ^{13}C NMR (101 MHz, CD_3OD, 298 K) δ 170.28, 138.44, 138.12, 133.81, 132.53, 132.06, 131.74, 131.12, 128.93, 126.84, 57.33, 28.37. HRMS (MALDI–TOF): calculated for $C_{24}H_{24}NO_4S_2$ $[M+H]^+$ *m/z* 476.1141, found 476.0284.

Table S1. Examples of small molecular fluorescence sensors for Pt^{2+} and Pt drugs in literature

Fluorescent probes	Probe Concentration	Detection parameters	Applications
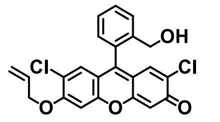 Fluorescein derivative **1**	12.5–300 μM	DMSO–pH 7 buffer (v/v = 1:4) λ_{ex} = 497 nm	Detection of total platinum content, different platinum species and cisplatin in serum samples (Ref [15])
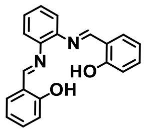 **L3**	10 μM	Air-saturated DMF or degassed DMF λ_{ex} = 400 nm or 525 nm	Phosphorescence detection of different Pt(II) sources and cisplatin (Ref [16])
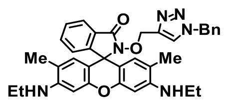 Rhodamine-Triazole Conjugate **1**	5 μM	H_2O/DMSO (v/v = 99:1) solution λ_{ex} = 500 nm	Detection of Pt(II) species including K_2PtCl_4, Pt(COD)Cl_2, $PtCl_2$ and cisplatin in aqueous solution (Ref [17])
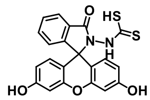 **FDCPt1**	100 μM	HEPES buffer (100 mM, pH 7.4, 50 % DMF λ_{ex} = 516 nm	Detection of monofunctional platinum species in several cell lines treated with cisplatin and oxaliplatin (Caco-2, HT29 and A549) (Ref [18])
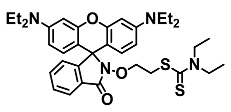 **Rho-DDTC**	20–30 μM	HEPES buffer (20 mM, pH 7.4, 30 % EtOH) λ_{ex} = 490 nm	Imaging of cisplatin and several Pt(IV) prodrugs in HeLa cells (Ref [19])
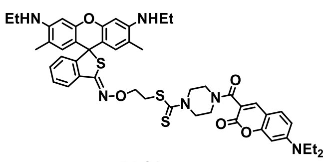 **RDC1**	20 μM	CH_3CN/HEPES buffer solution (v/v = 7:3, 5 mM, pH 7.4) λ_{ex} = 400 nm	HeLa cells treated with various Pt(IV) complexes. Buthionine-sulfoximine (BSO) treated cells showed GSH is not the dominant cellular reductant of Pt(IV) prodrug complexes (Ref [20])
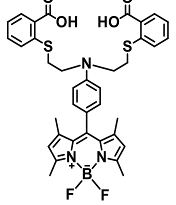 **PS** This work	5–10 μM	DMF/HEPES buffer solution (v/v = 3:7, 10 mM, pH 7.2) DMF/water solution (v/v = 1:9, pH = 7) λ_{ex} = 500 nm	Imaging and detection of Pt^{2+}, organoplatinum drugs like cisplatin and nedaplatin in A549 lung carcinomas

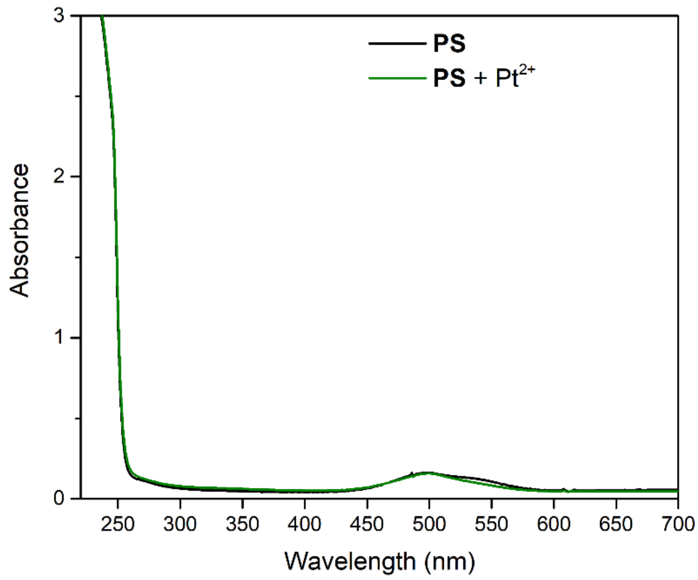

Figure S1. UV–visible absorption spectra of **PS** (5 μM) upon addition of Pt^{2+} (20 mol equiv.). Conditions: DMF–HEPES (*v/v* = 3:7, 10 mM, pH = 7.2, 25 °C).

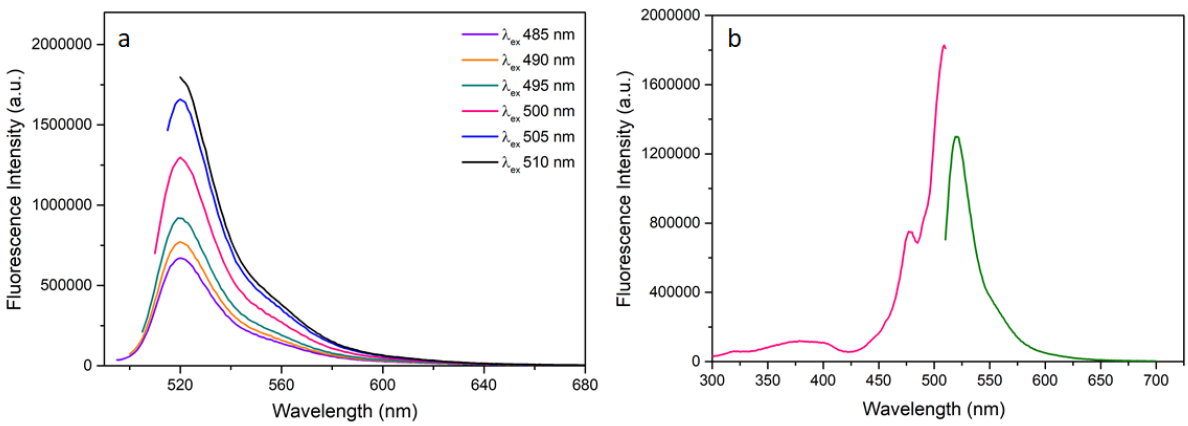

Figure S2. (a) Emission spectra of **PS** (5 μM) upon reacting with Pt^{2+} (20 mol equiv.) using different excitation wavelengths from 485 nm to 510 nm. Conditions: DMF–HEPES buffer (*v/v* = 3:7, 10 mM, pH = 7.2). (b) Excitation spectrum and emission spectrum of **PS** (5 μM) upon reacting with Pt^{2+} (20 mol equiv.). λ_{ex} = 500 nm and λ_{em} = 520 nm.

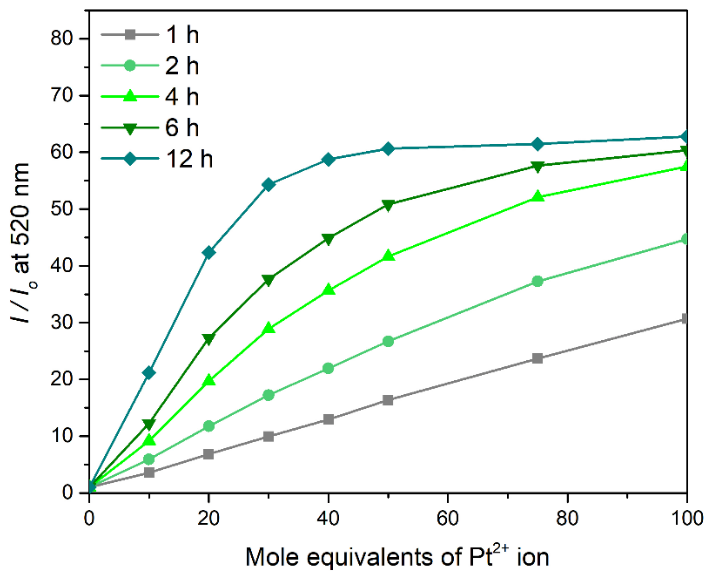

Figure S3. Time dependent fluorescence response of **PS** (5 μM) upon addition of Pt^{2+} (0–100 mol equiv.). Conditions: DMF–HEPES (v/v = 3:7, 10 mM, pH = 7.2, 25 °C), λ_{ex} = 500 nm.

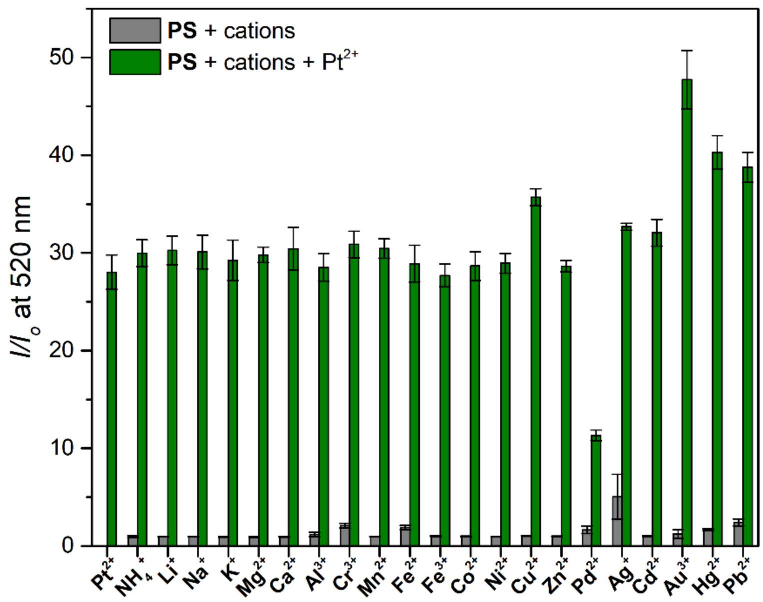

Figure S4. Relative fluorescence response (I/I_o) of **PS** (5 μM) to Pt^{2+} in the presence of various cations (20 mol equiv.). Conditions: DMF–HEPES buffer solution (v/v = 3:7, 10 mM, pH = 7.2, 25 °C), λ_{ex} = 500 nm, n = 3.

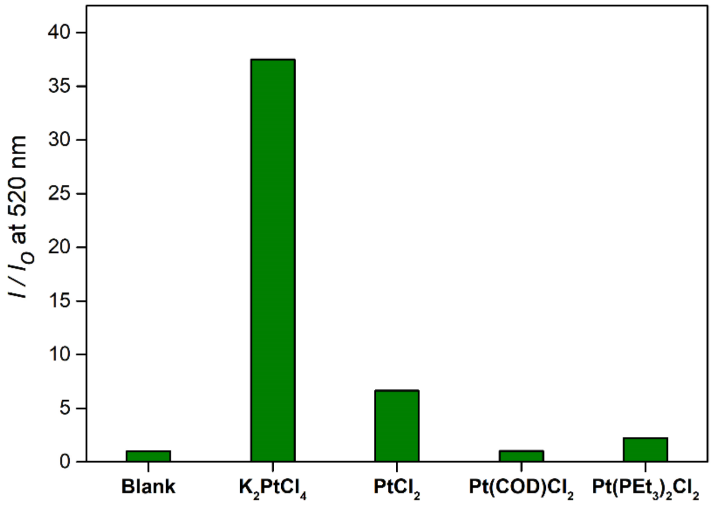

Figure S5. Fluorescence response (I/I_o) of **PS** (5 μM) in the presence of Pt(II) complexes (20 mol equiv.). Conditions: DMF–HEPES (v/v = 3:7, 10 mM, pH = 7.2, 25 °C), λ_{ex} = 500 nm.

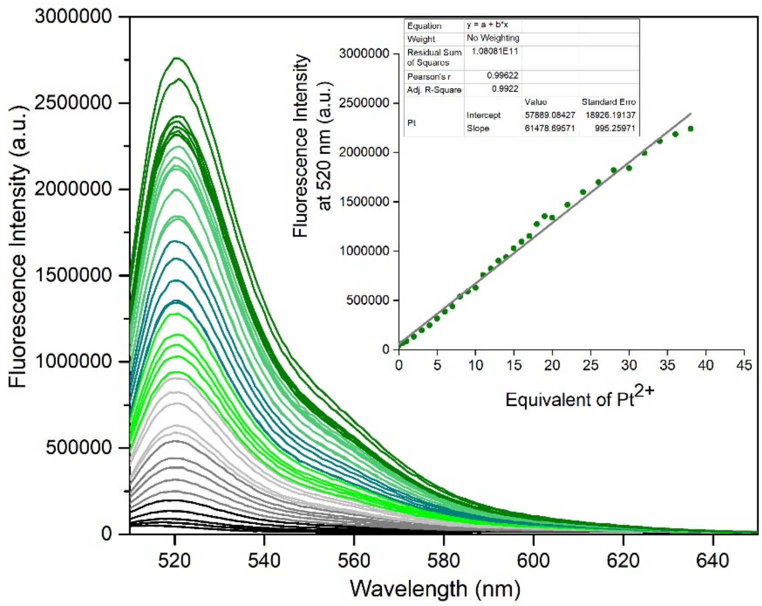

Figure S6. Fluorescence titration of **PS** (5 μM) in the presence of Pt^{2+} (0, 0.5, 1.0, 2.0, 3.0, 4.0, 5.0, 6.0, 7.0, 8.0, 9.0, 10.0, 11.0, 12.0, 13.0, 14.0, 15.0, 16.0, 17.0, 18.0, 19.0, 20.0, 22.0, 24.0, 26.0, 28.0, 30.0, 32.0, 34.0, 36.0, 38.0, 40.0, 42.0, 44.0, 46.0, 48.0, 50.0, 75.0, 100.0 mol equiv.). Inset: linear correlation between the fluorescence intensity at 520 nm and concentration of Pt^{2+} (0–40 mol equiv.). Condition: DMF–HEPES buffer (v/v = 3:7, 10 mM, pH = 7.2), λ_{ex} = 500 nm.

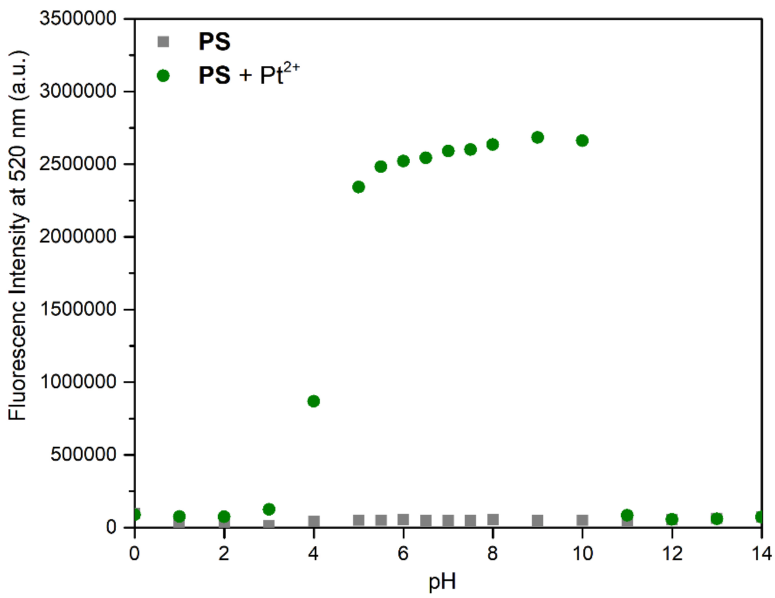

Figure S7. Effect of pH on the fluorescence intensity of **PS** (5 μM) in the absence or presence of Pt^{2+} (20 mol equiv.). Conditions: DMF–water solution (*v/v* = 3:7, pH = 0.0, 1.0, 2.0, 3.0, 4.0, 5.0, 5.5, 6.0, 6.5, 7.0, 7.5, 8.0, 9.0, 10.0, 11.0, 12.0, 13.0 and 14.0, 25 °C), λ_{ex} = 500 nm. The pH of aqueous solution was tuned with HCl and NaOH.

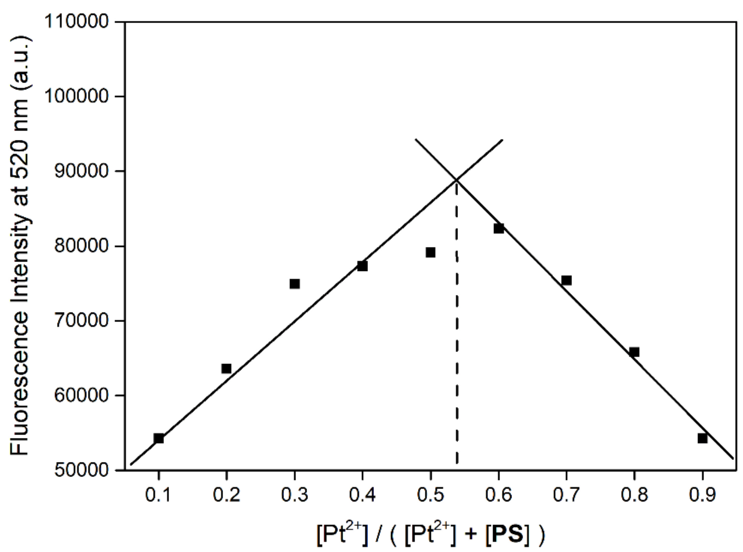

Figure S8. Job's plot of **PS** responding to Pt^{2+}. The total concentration of **PS** and Pt^{2+} is 10 μM. Conditions: DMF–HEPES buffer solution (*v/v* = 3:7, 10 mM, pH 7.2, 25 °C), λ_{ex} = 500 nm.

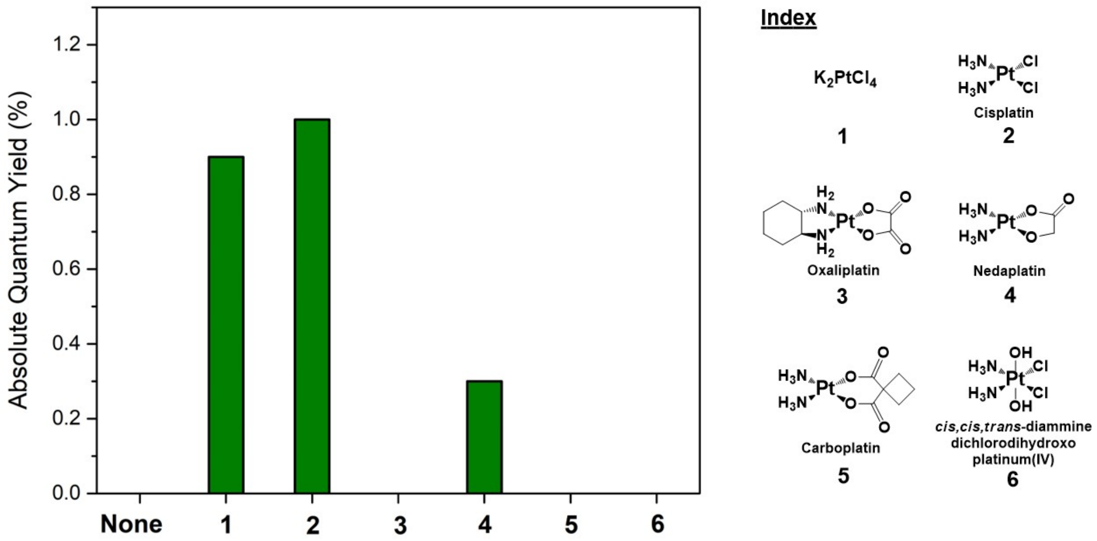

Figure S9. Absolute photoluminescence quantum yields of **PS** (5 μM) upon addition of different Pt complexes (20 mol equiv.). Conditions: DMF–water solution (*v/v* = 1:9, pH = 7, 25 °C), incubation for 12 h, λ_{ex} = 500 nm. The corresponding complex structures and names are shown in index for reference.

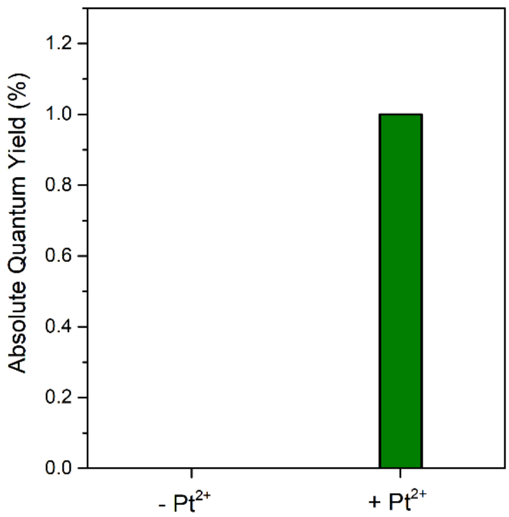

Figure S10. Absolute photoluminescence quantum yields of **PS** (5 μM) in the absence and the presence of Pt^{2+} (20 mol equiv.). Conditions: DMF–HEPES (*v/v* = 3:7, 10 mM, pH = 7.2, 25 °C), incubation for 6 h, λ_{ex} = 500 nm.

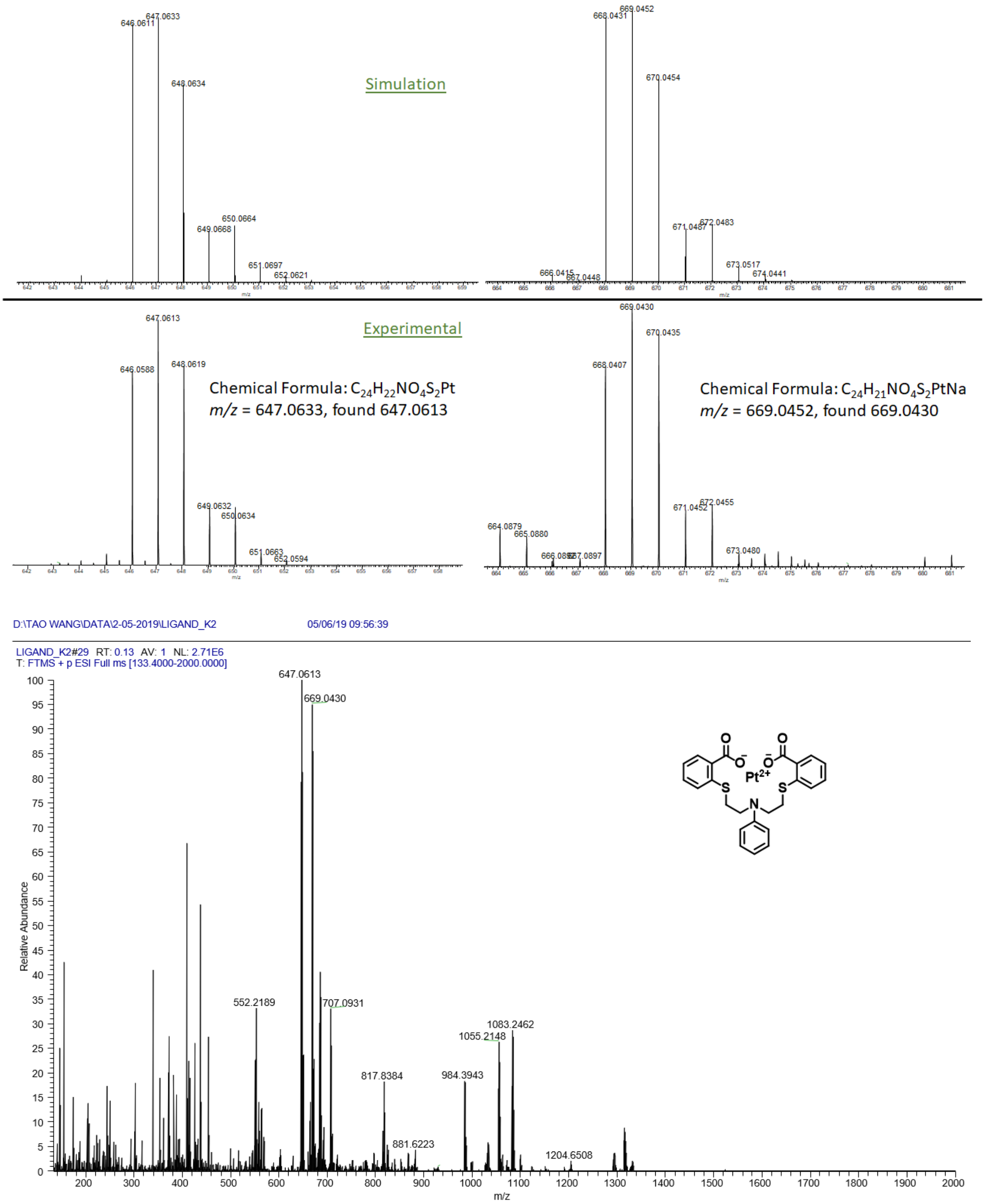

Figure S11. HRMS (ESI) spectrum of platinum complex ensemble [**L**–H+Pt]$^+$ and [**L**–2H+Pt+Na]$^+$ from reaction mixture of K_2PtCl_4 and compound **L**. Top: enlarged peaks of the mass spectrum and bottom: scan of the mass spectrum.

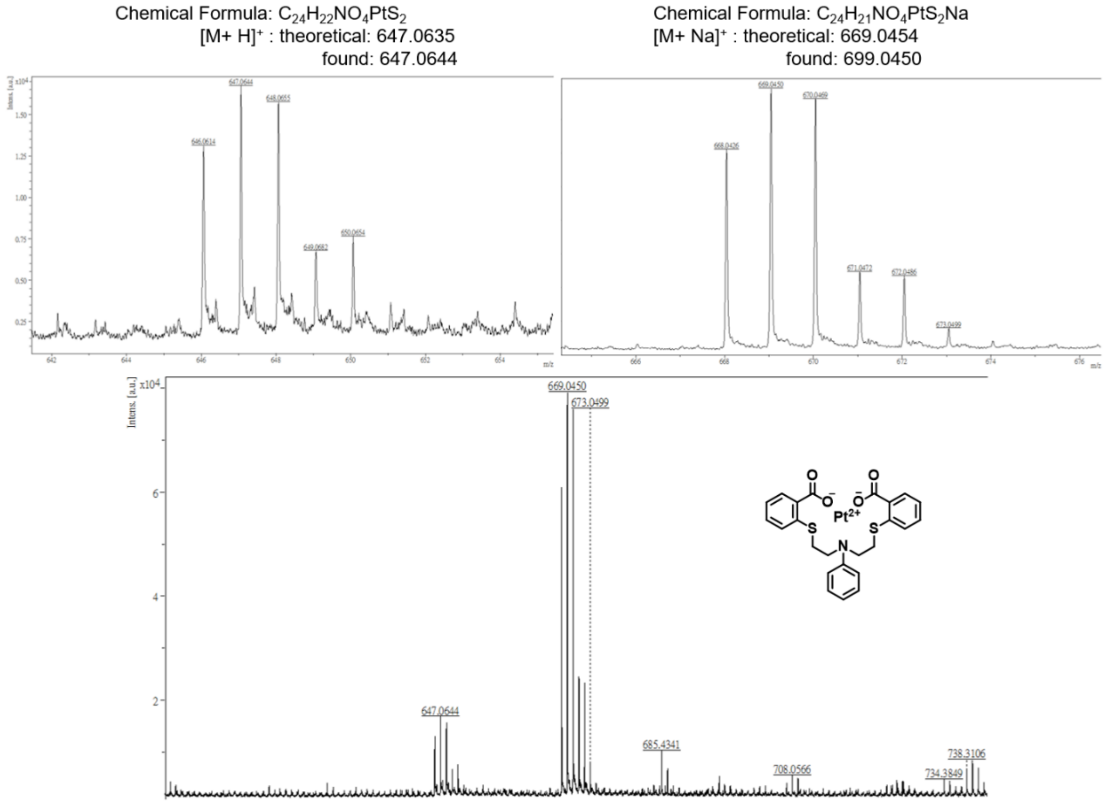

Figure S12. HRMS (MALDI–TOF) spectrum of platinum complex ensemble [**L**–H+Pt]$^{+}$ and [**L**–2H+Pt+Na]$^{+}$ from reaction mixture of cisplatin and compound **L**. Top: enlarged peaks of the mass spectrum with the isotopic patterns and bottom: scan of the mass spectra.

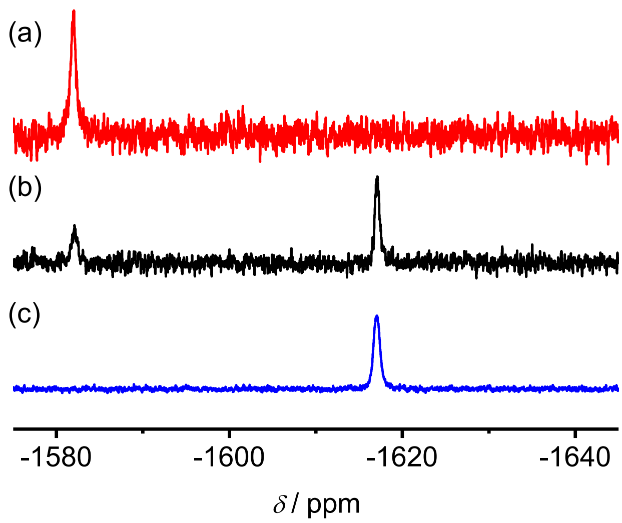

Figure S13. (a) ^{195}Pt NMR spectra of compound **L** in CD_3OD with the addition of 1 mol equiv. of K_2PtCl_4 in NaOD solution in D_2O (δ = –1582 ppm); (b) ^{195}Pt NMR spectra of the sample in (a) with K_2PtCl_4 in D_2O (δ = –1617 ppm) in sealed capillary tube as external reference; (c) ^{195}Pt NMR spectra of K_2PtCl_4 in D_2O.

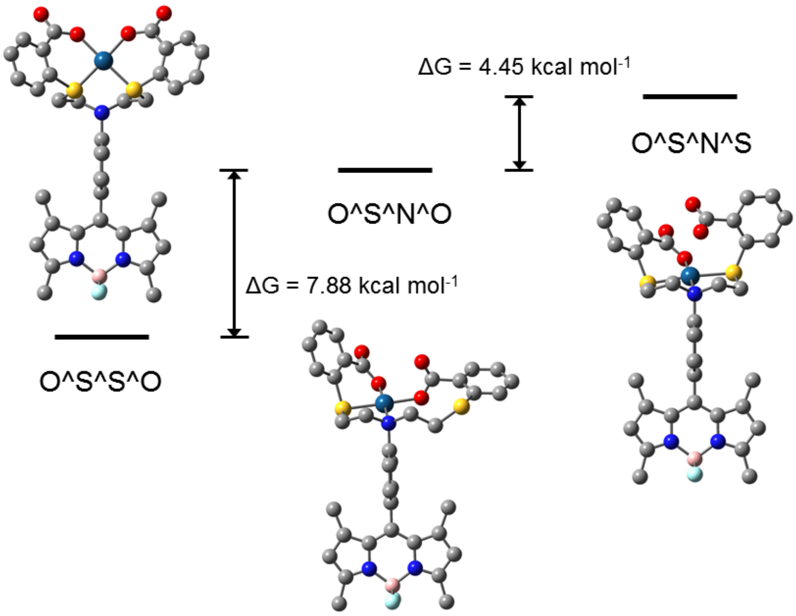

Figure S14. Schematic energy profile of the three conformations of **PS+Pt^{2+}** obtained at the PBE0 level of theory.

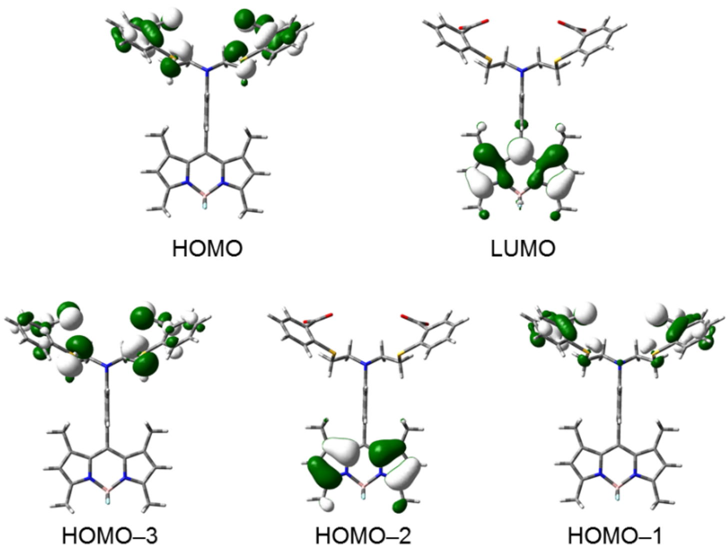

Figure S15. Spatial plots (isovalue = 0.03) of frontier molecular orbitals of the fluorescent sensor **PS** at the optimized PBE0 ground-state geometry.

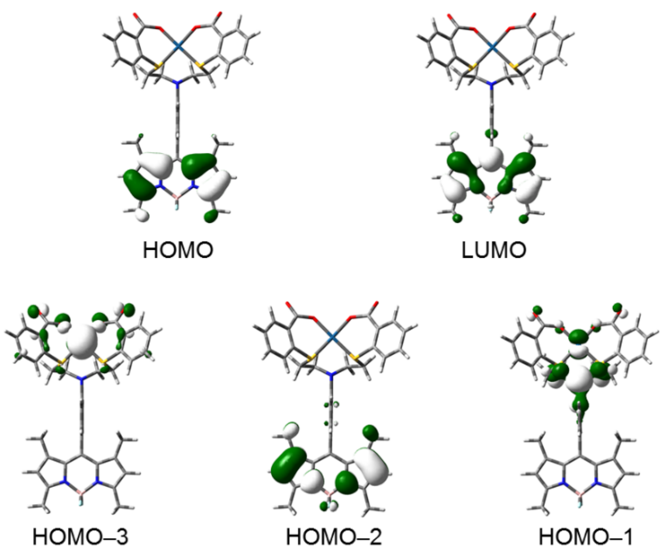

Figure S16. Spatial plots (isovalue = 0.03) of frontier molecular orbitals of **PS+Pt^{2+}**, in the O^S^S^O binding mode, at the optimized PBE0 ground-state geometry.

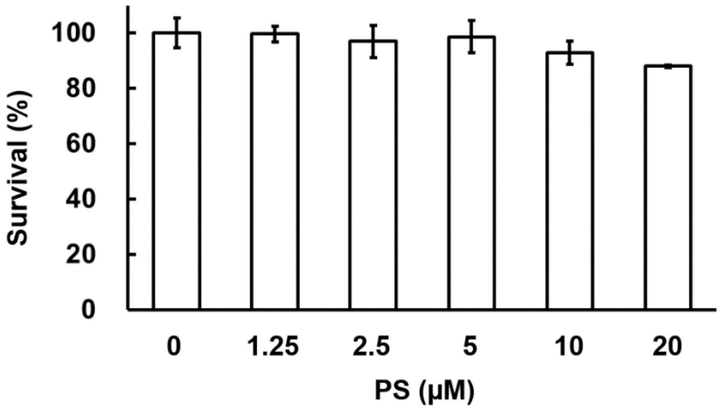

Figure S17. MTT cytotoxicity assay of **PS** at different concentrations on A549 cells.

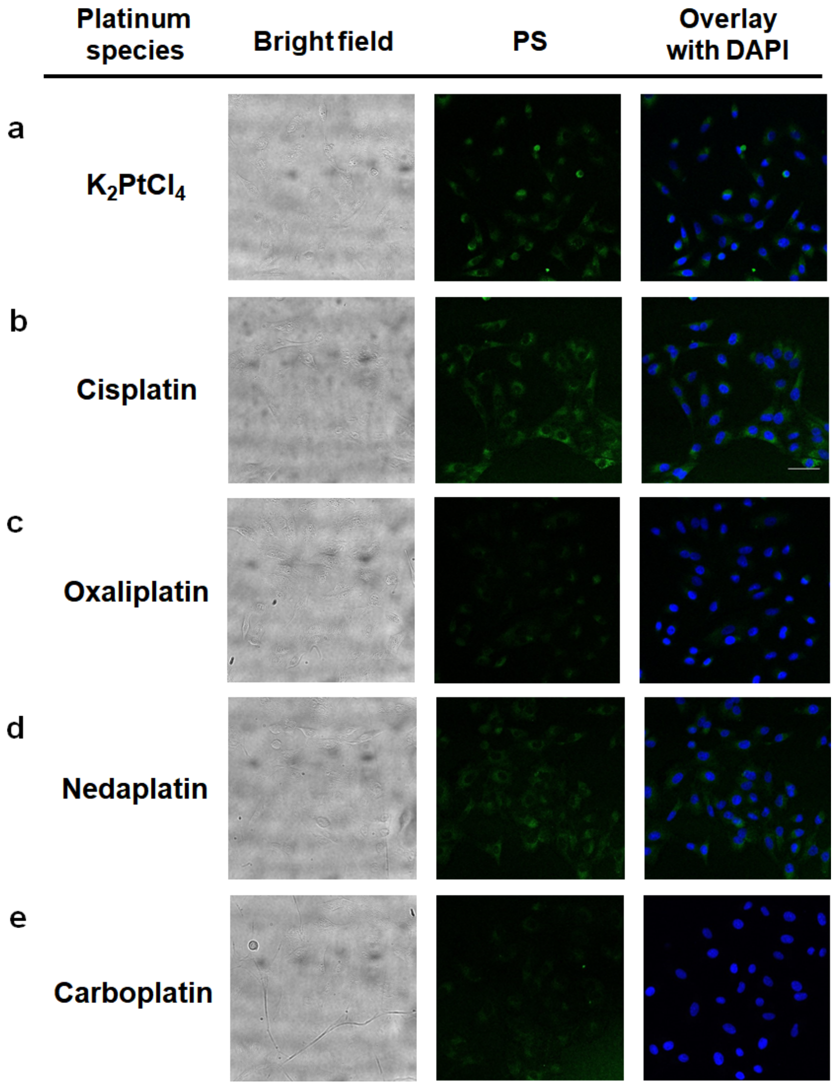

Figure S18. Confocal laser scanning microscopic images (CLSM) of A549 cells. Cells were exposed with different platinum species (10 μM) for 4 h and then incubated with **PS** (10 μM) for 30 min at 37 °C. (a) K_2PtCl_4; (b) cisplatin; (c) oxaliplatin; (d) nedaplatin and (e) carboplatin. Scale bar represents 50 μm.

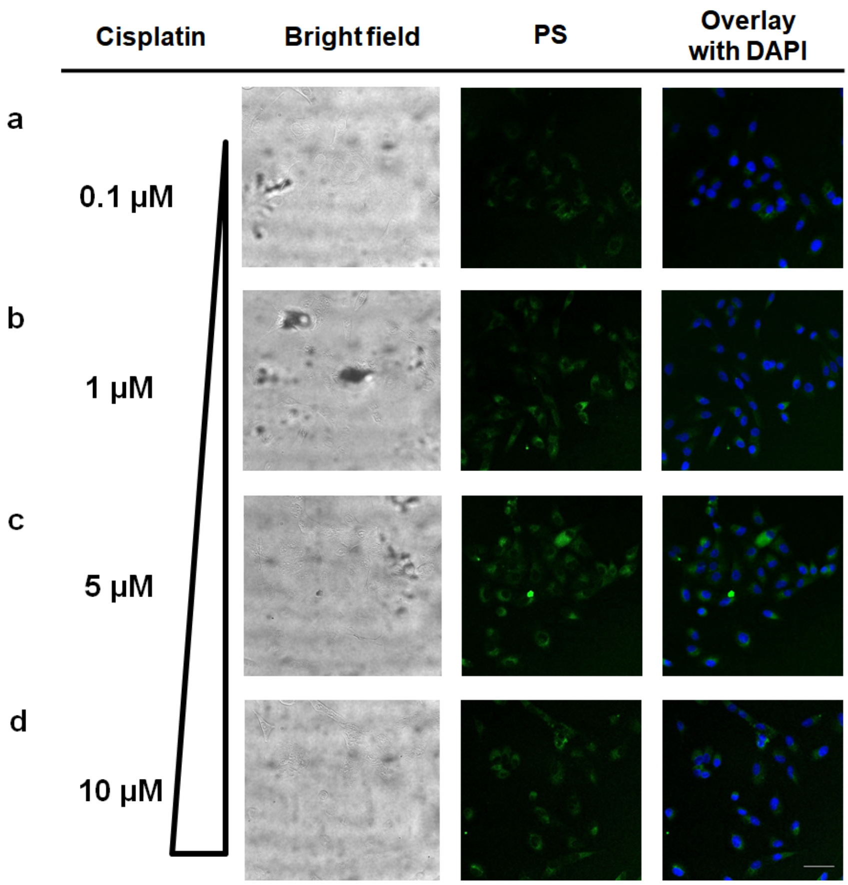

Figure S19. Confocal laser scanning microscopic images (CLSM) of A549 cells. Cells were exposed with different concentration of cisplatin (0.1–10 μM) for 4 h and then incubated with **PS** (10 μM) for 30 min at 37 °C. (a) 0.1 μM; (b) 1 μM; (c) 5 μM and (d) 10 μM of cisplatin. Scale bar represents 50 μm.

NMR Spectra

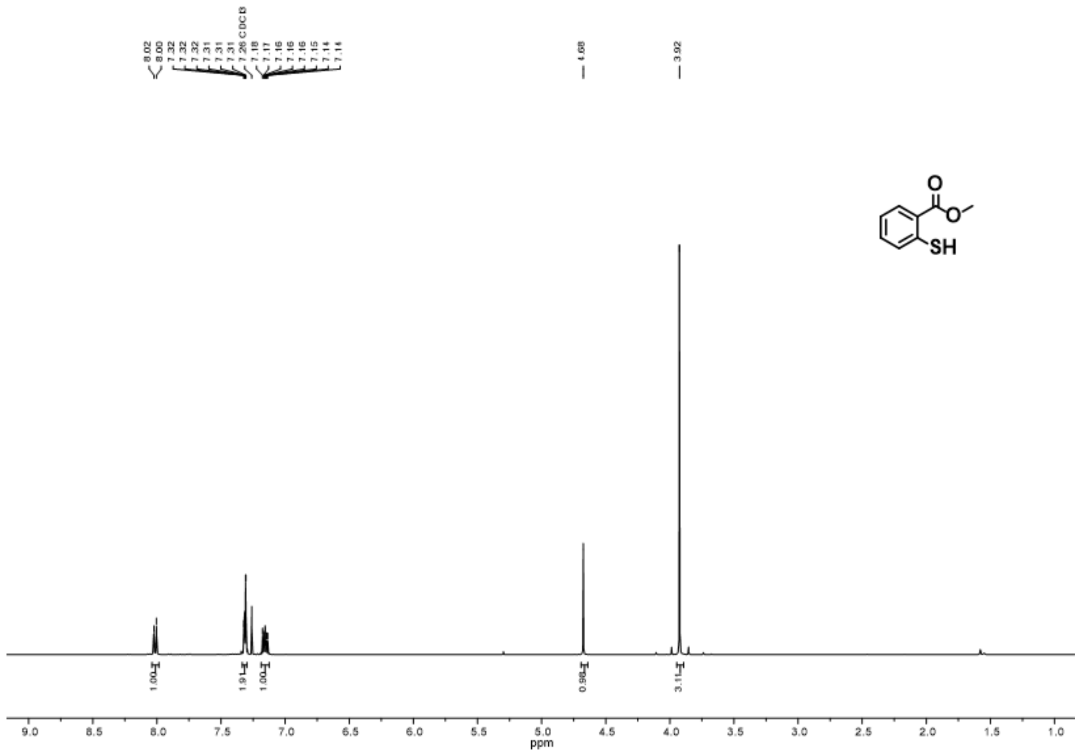

Figure S20. ^{1}H NMR spectrum (400 MHz, $CDCl_3$, 298 K) of compound **7**.

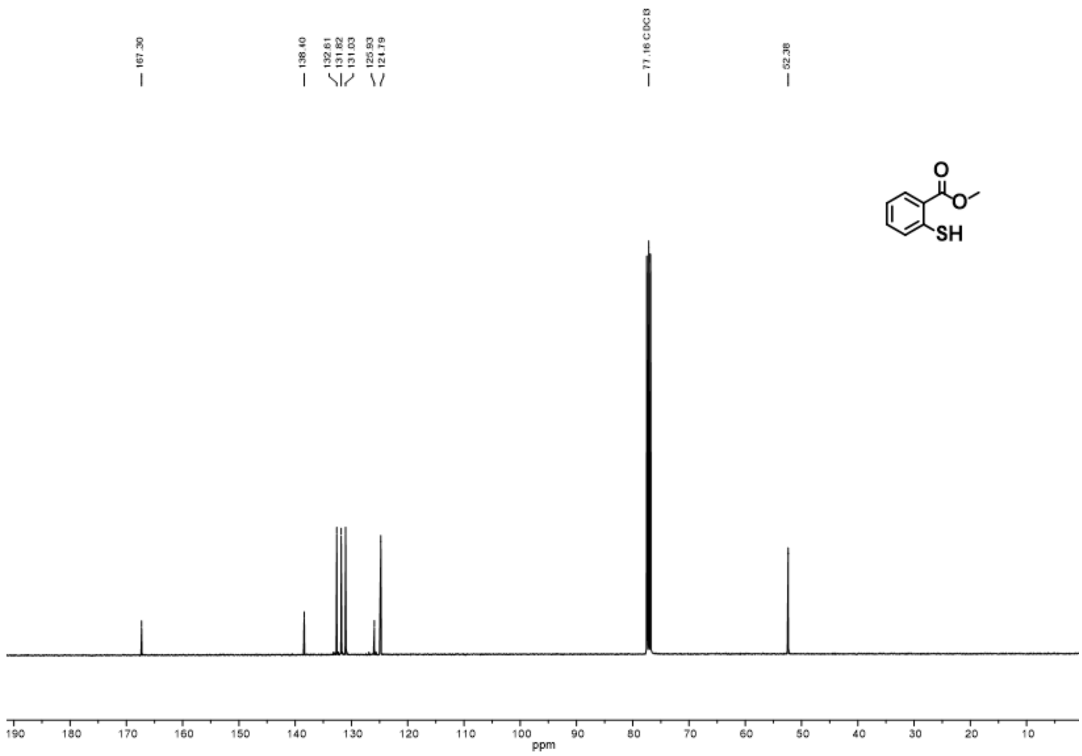

Figure S21. $^{13}C\{^{1}H\}$ NMR spectrum (101 MHz, $CDCl_3$, 298 K) of compound **7**.

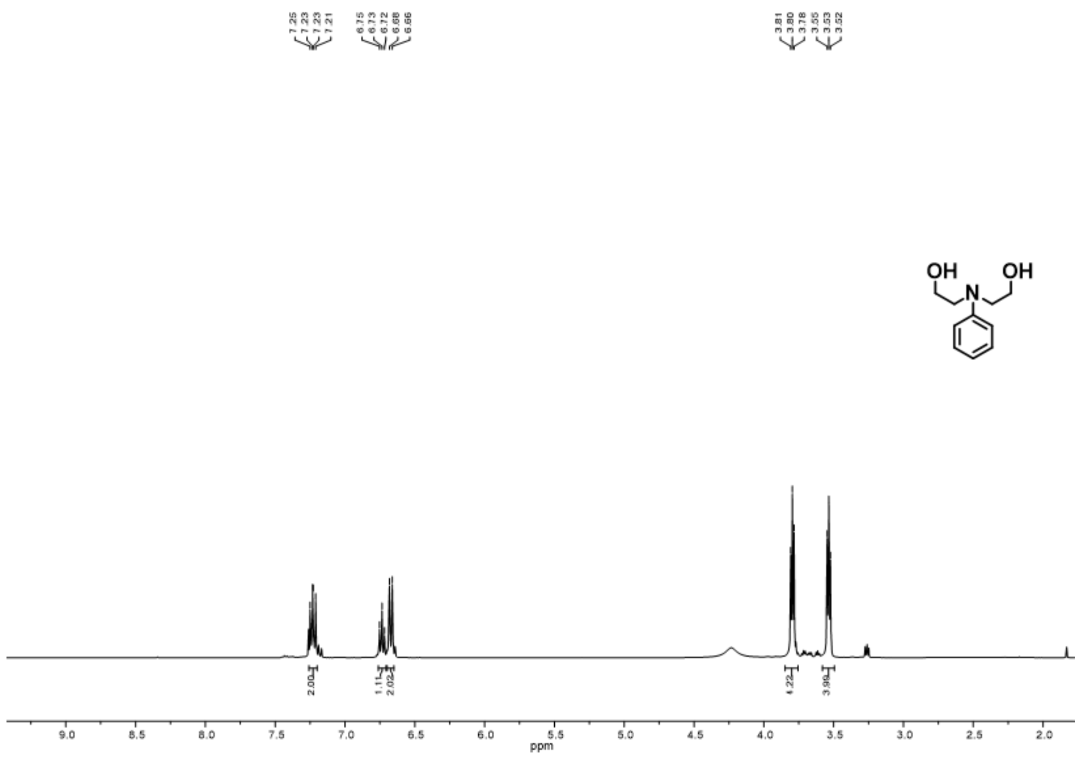

Figure S22. ^{1}H NMR spectrum (400 MHz, $CDCl_3$, 298 K) of compound **8**.

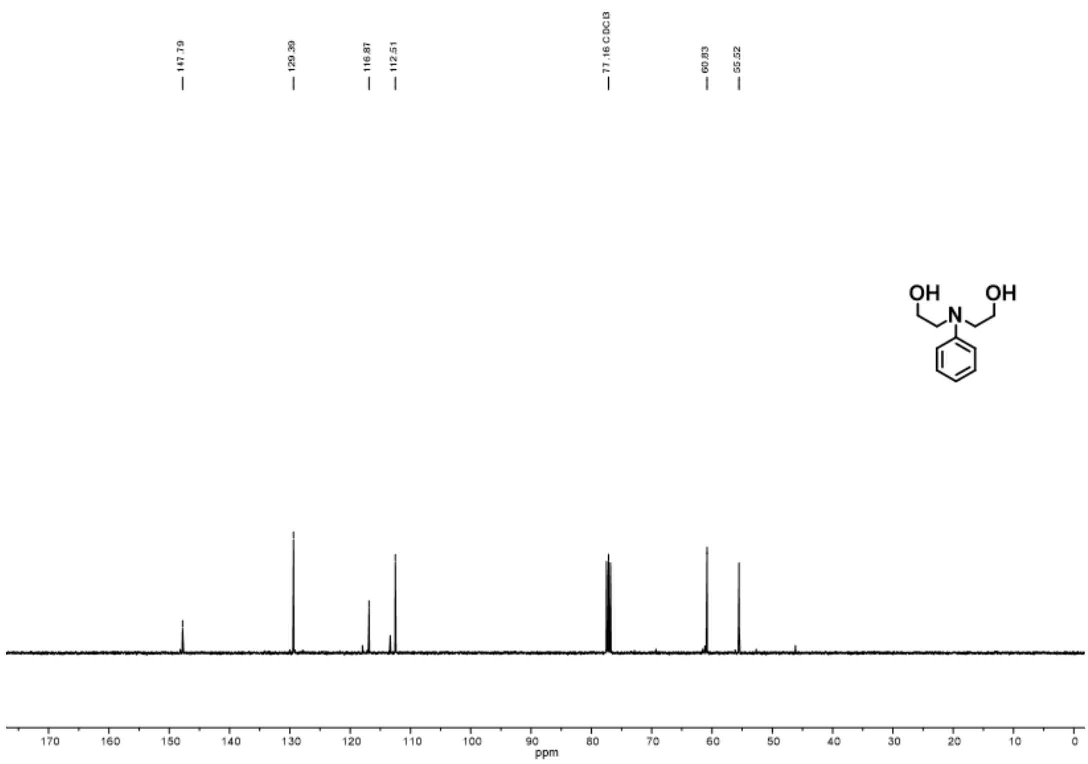

Figure S23. $^{13}C\{^{1}H\}$ NMR spectrum (101 MHz, $CDCl_3$, 298 K) of compound **8**.

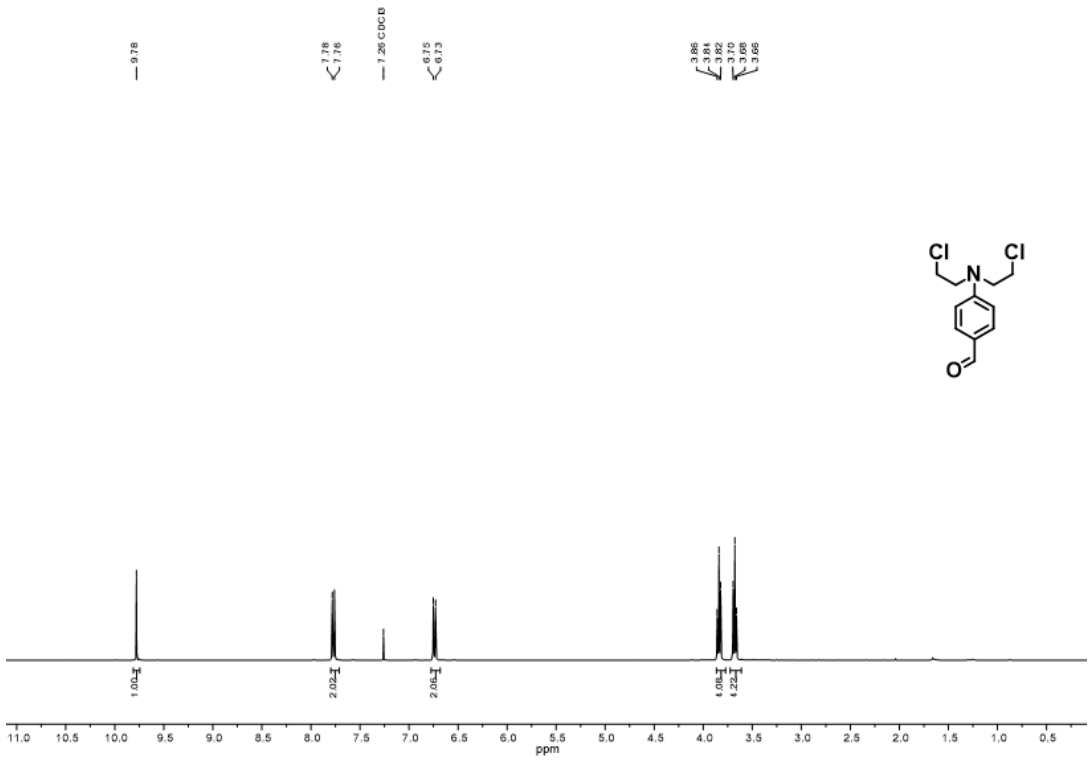

Figure S24. ^{1}H NMR spectrum (400 MHz, $CDCl_3$, 298 K) of compound **9**.

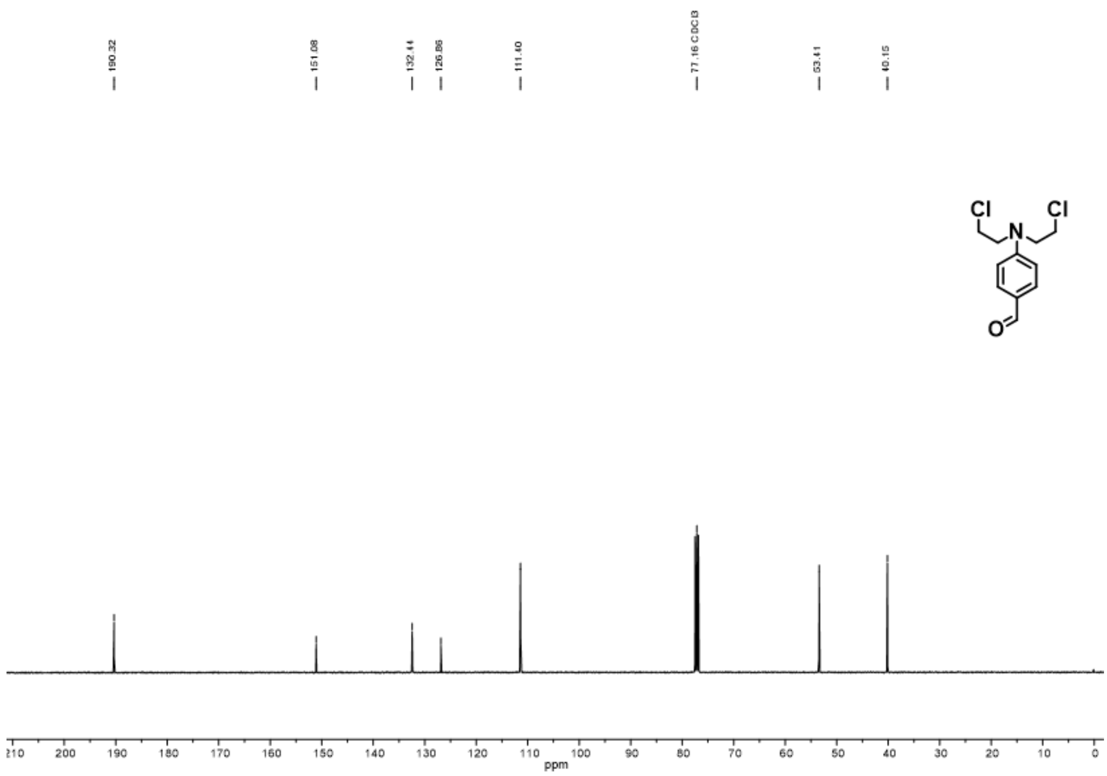

Figure S25. $^{13}C\{^{1}H\}$ NMR spectrum (101 MHz, $CDCl_3$, 298 K) of compound **9**.

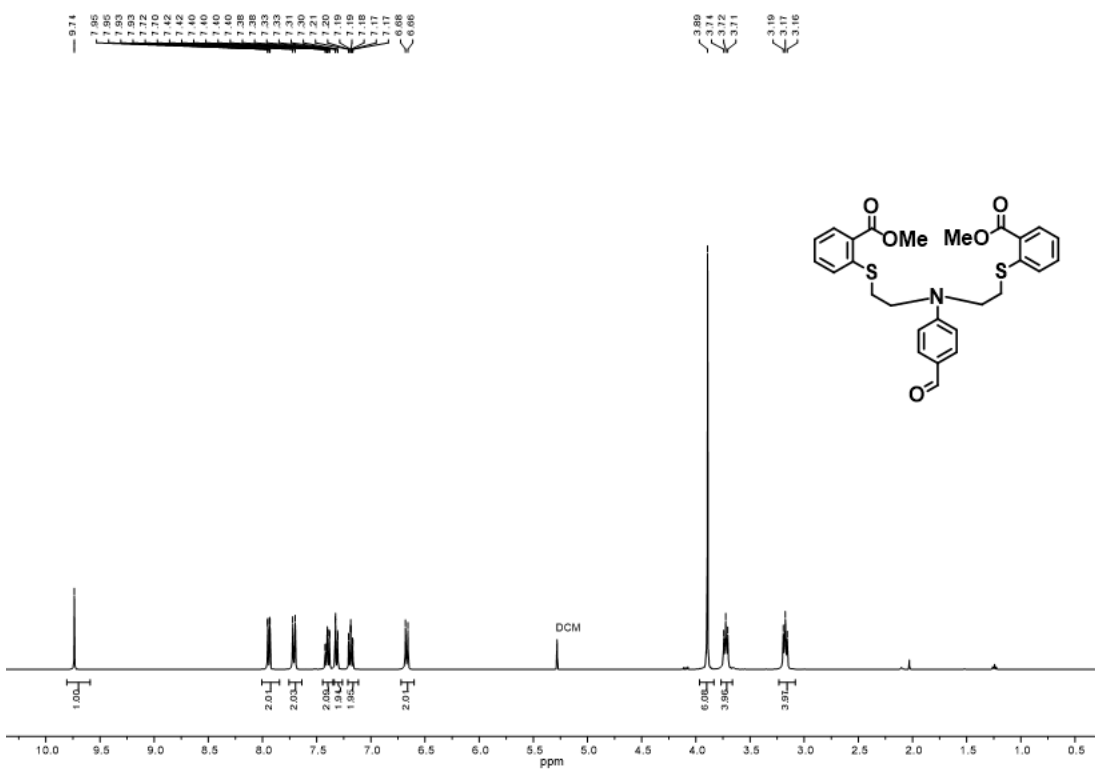

Figure S26. ^{1}H NMR spectrum (400 MHz, $CDCl_3$, 298 K) of compound **10**.

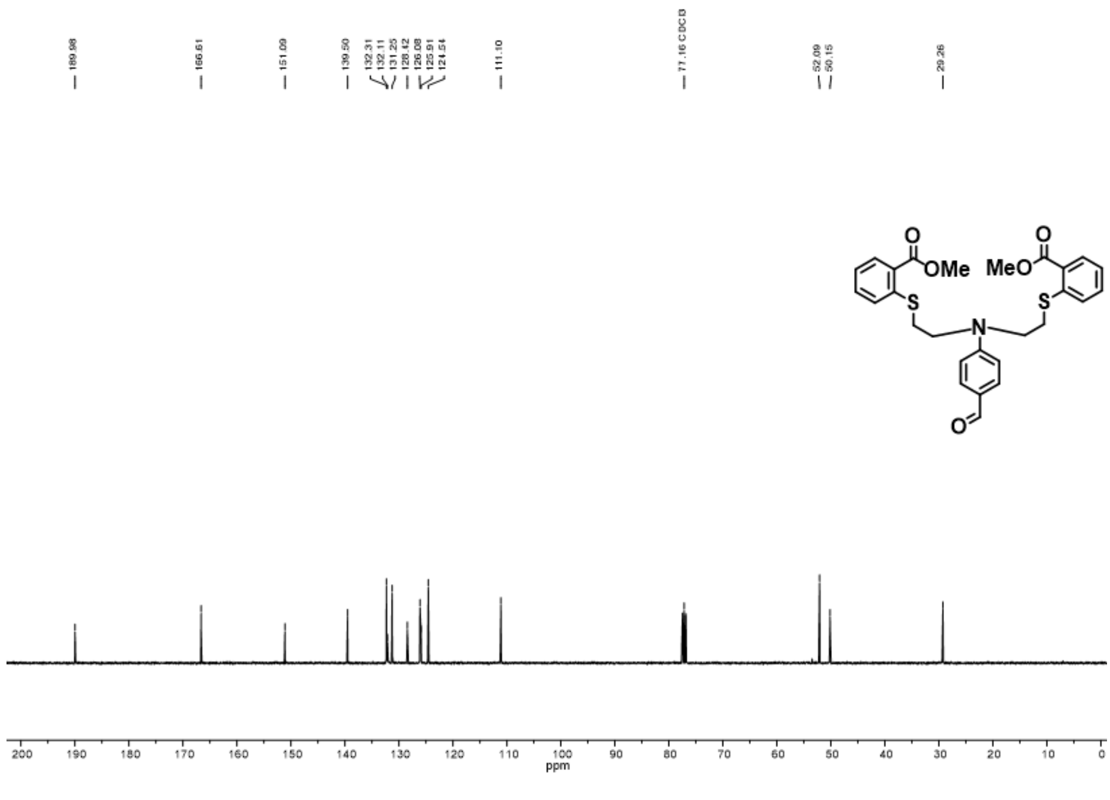

Figure S27. $^{13}C\{^{1}H\}$ NMR spectrum (101 MHz, $CDCl_3$, 298 K) of compound **10**.

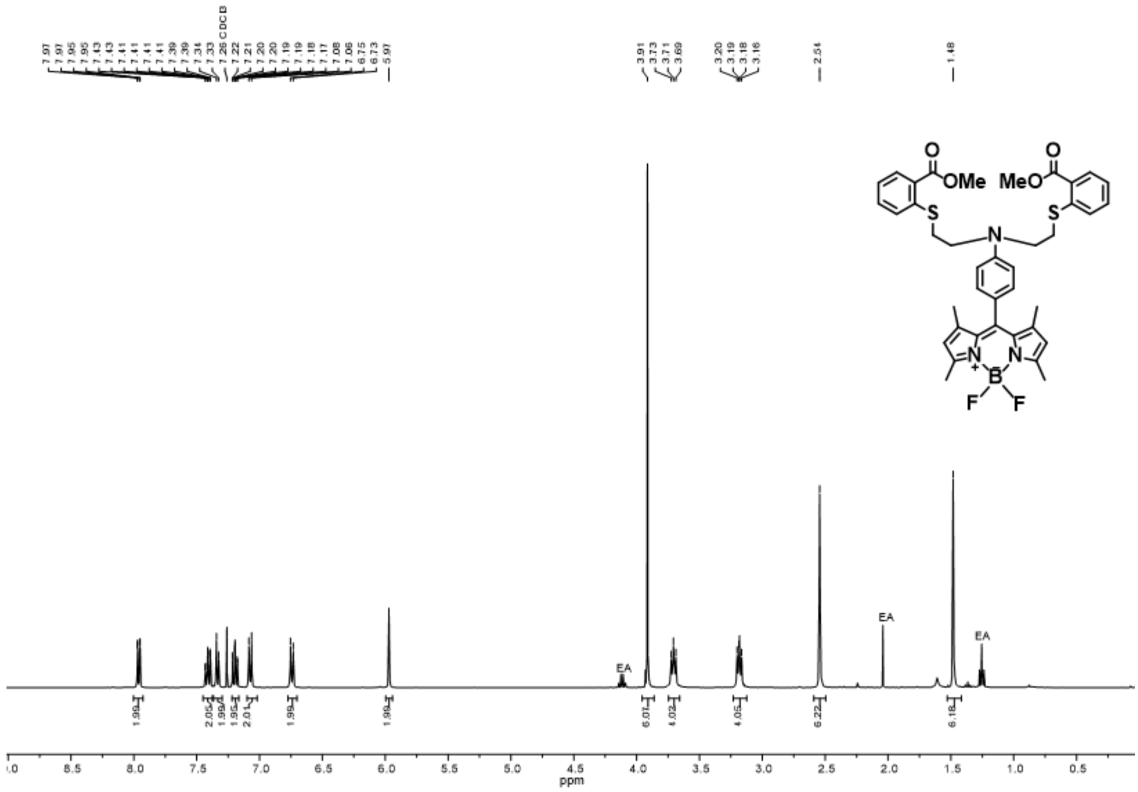

Figure S28. ^{1}H NMR spectrum (400 MHz, $CDCl_3$, 298 K) of compound **11**.

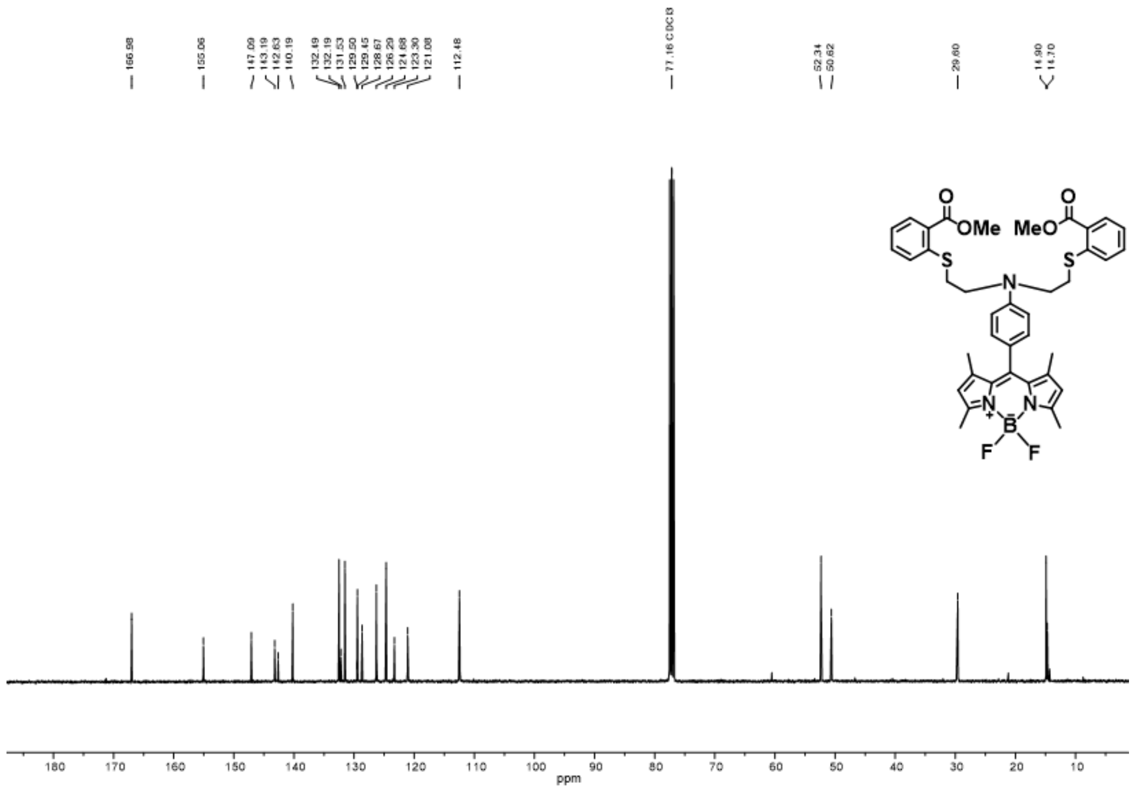

Figure S29. $^{13}C\{^{1}H\}$ NMR spectrum (101 MHz, $CDCl_3$, 298 K) of compound **11**.

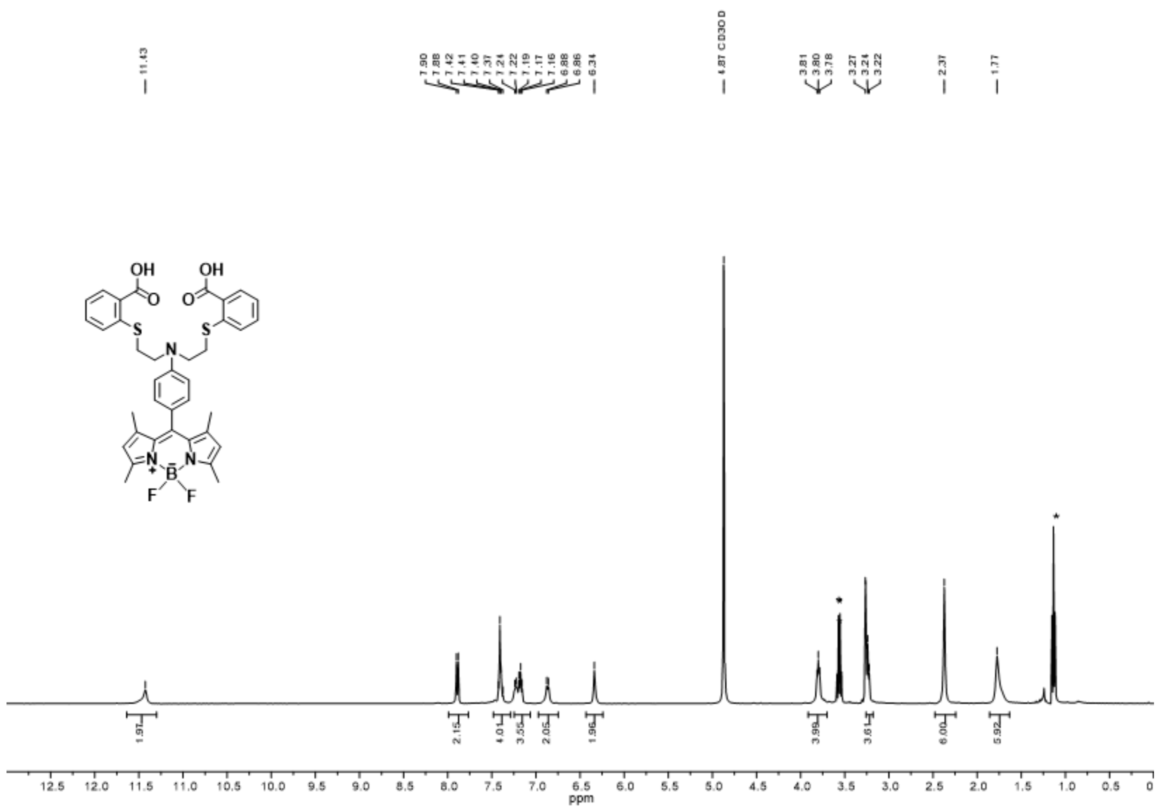

Figure S30. ^{1}H NMR spectrum (400 MHz, CD_3OD, 298 K) of **PS**.

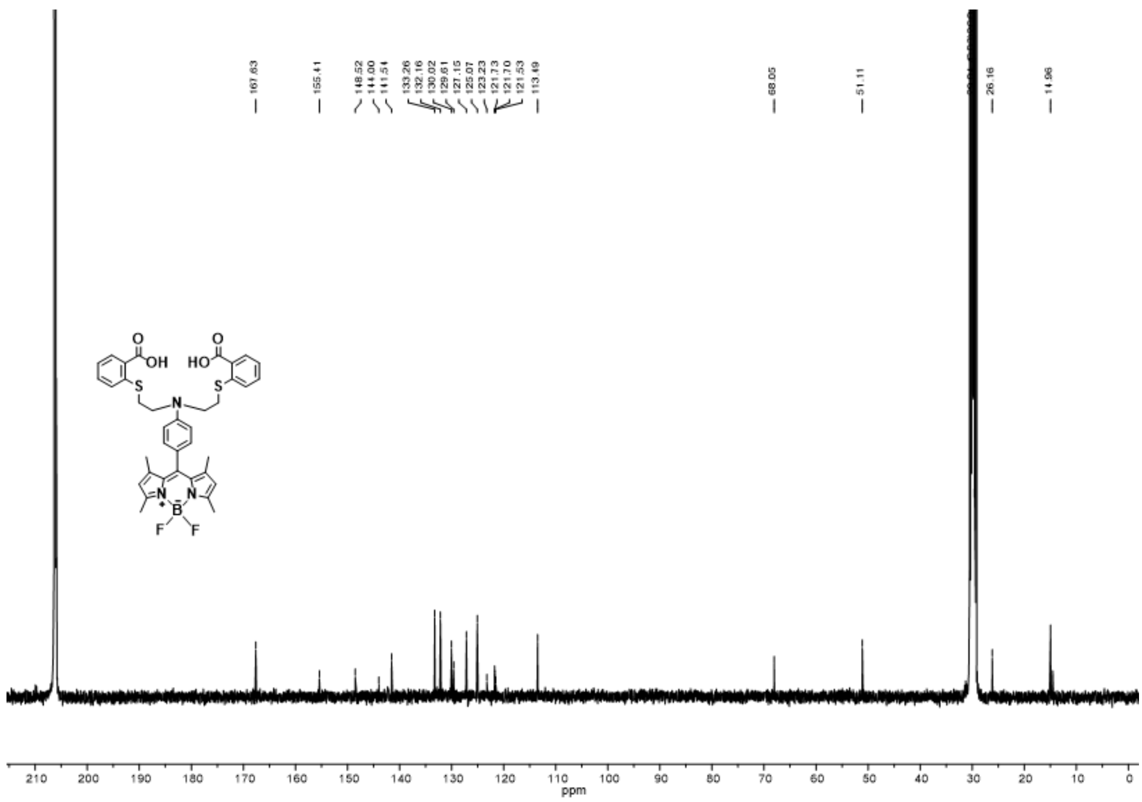

Figure S31. $^{13}C\{^{1}H\}$ NMR spectrum (101 MHz, $(CD_3)_2CO$, 298 K) of **PS**.

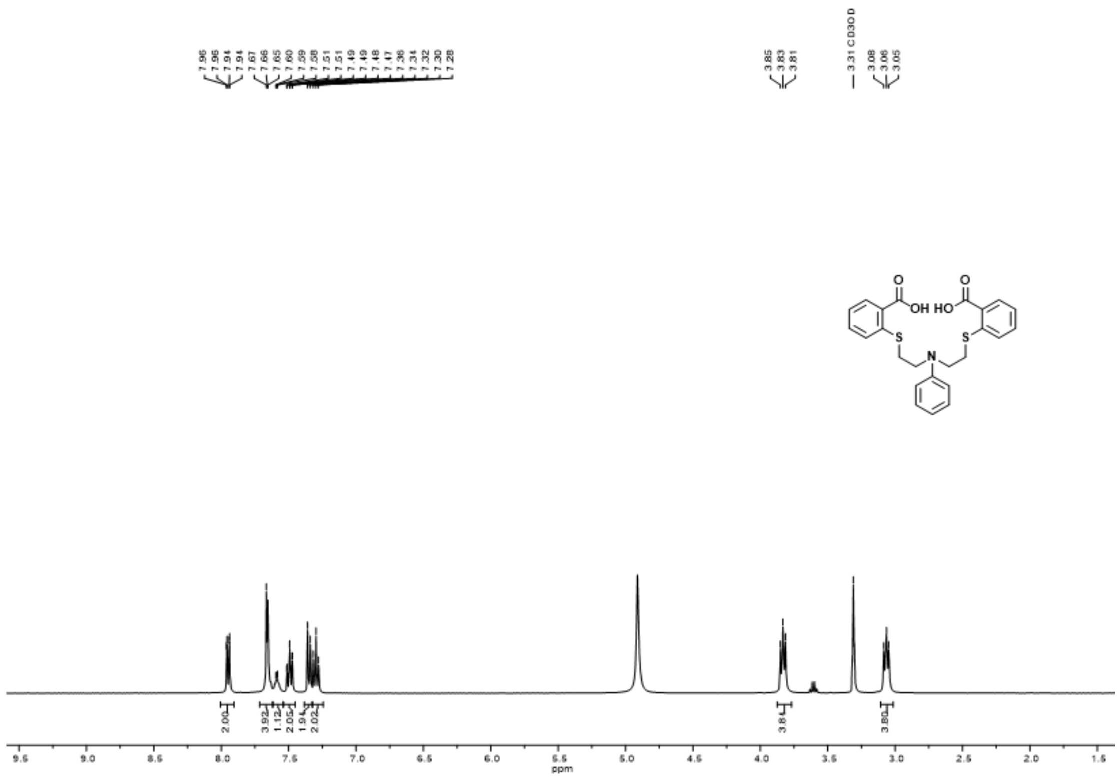

Figure S32. ^{1}H NMR spectrum (400 MHz, CD_3OD, 298 K) of compound **L**.

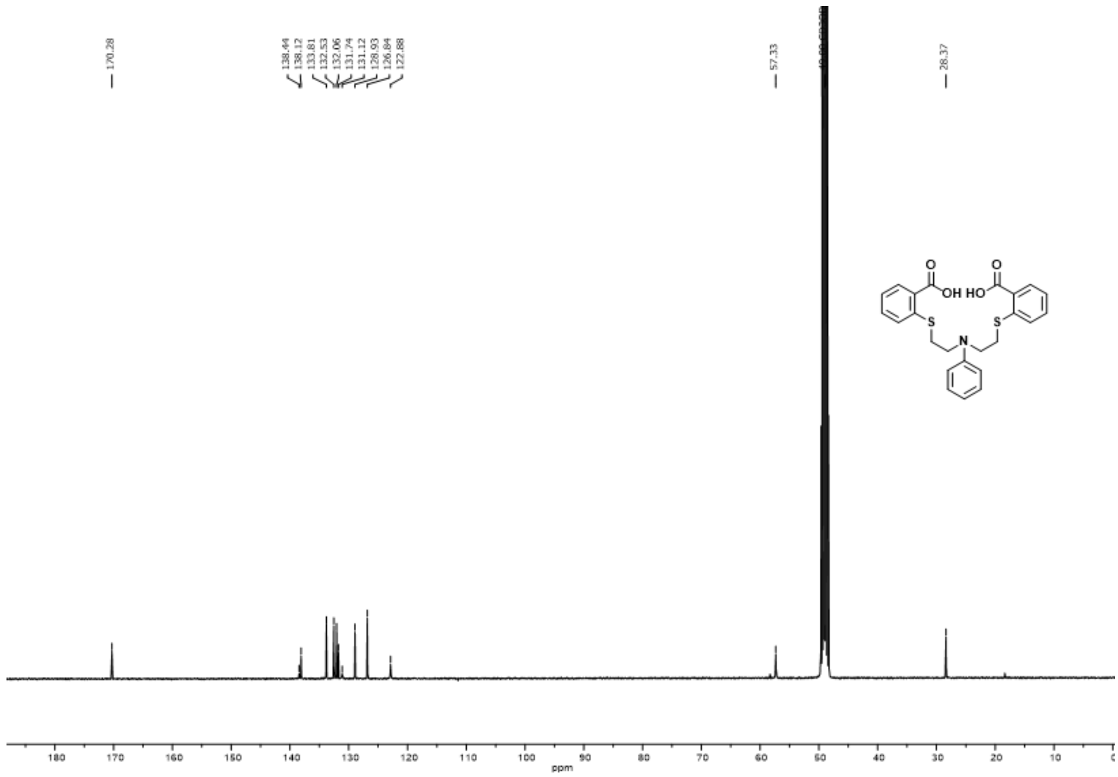

Figure S33. $^{13}C\{^{1}H\}$ NMR spectrum (101 MHz, CD_3OD, 298 K) of compound **L**.

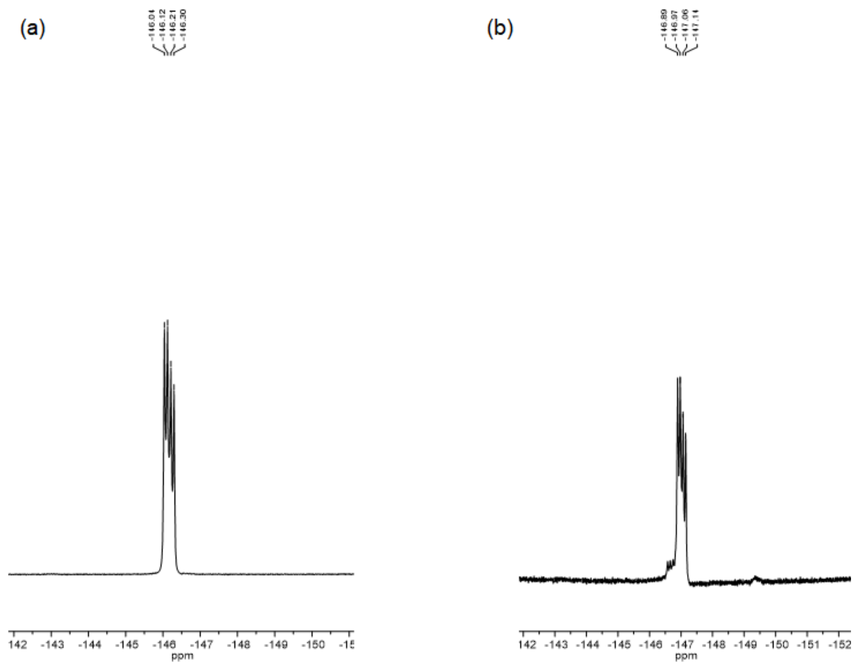

Figure S34. (a) ^{19}F NMR spectrum (377 MHz, $CDCl_3$, 298K) of compound **11** and (b) ^{19}F NMR spectrum (377 MHz, CD_3OD, 298K) of **PS**.

Mass spectra

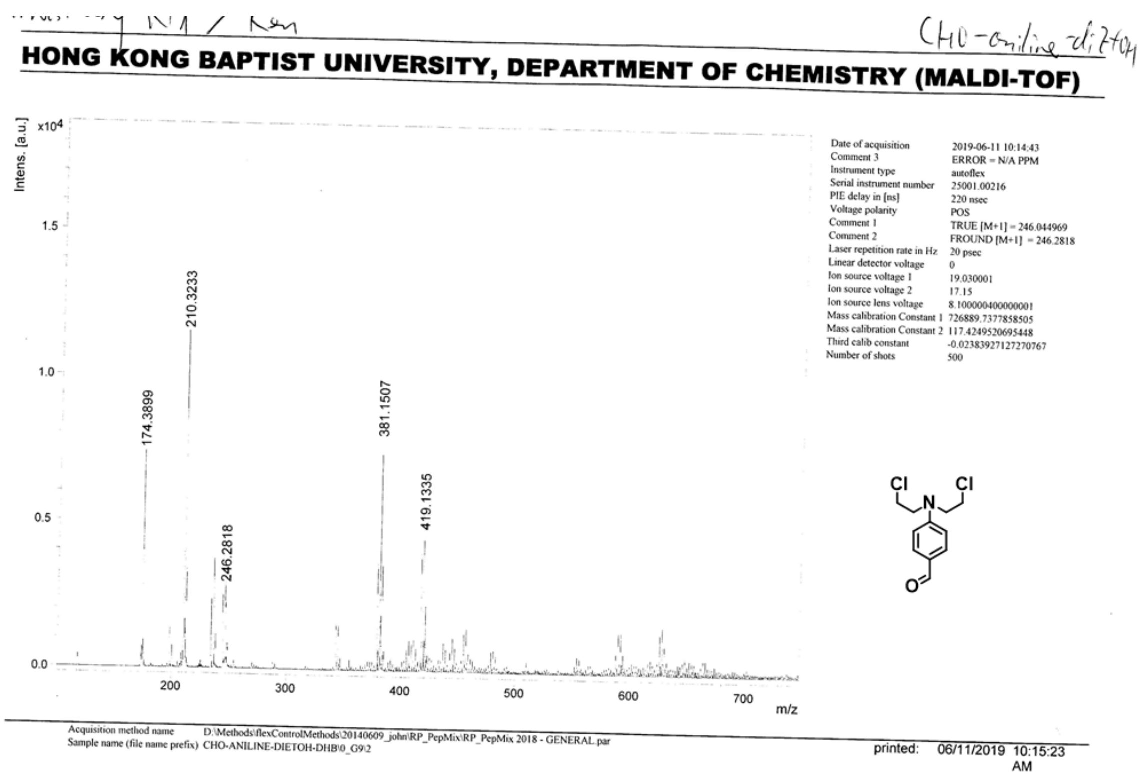

Figure S35. HRMS (MALDI–TOF) spectrum of compound **9**.

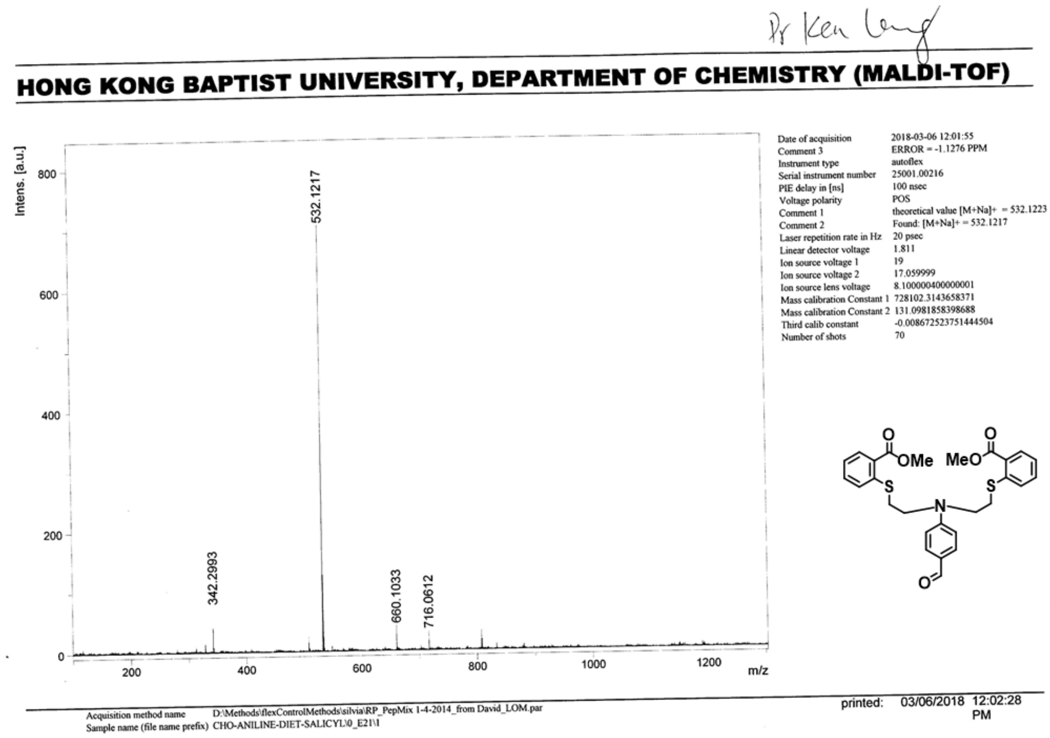

Figure S36. HRMS (MALDI–TOF) spectrum of compound **10**.

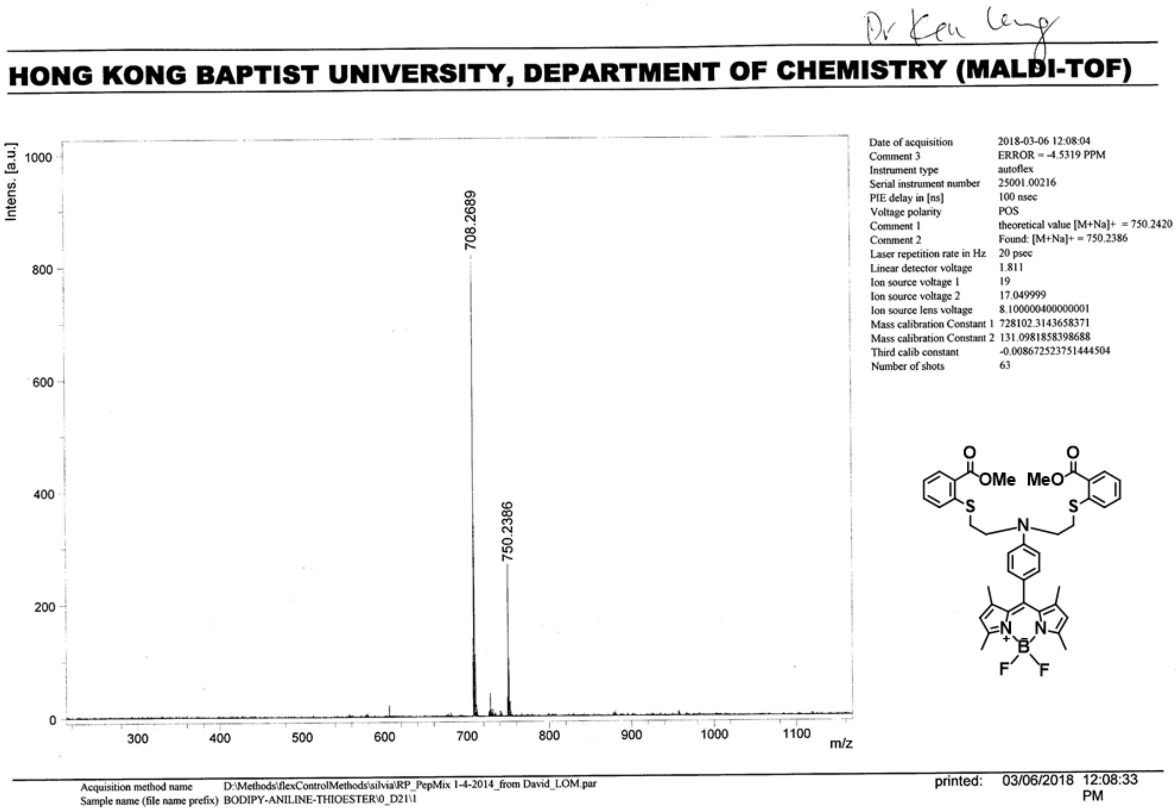

Figure S37. HRMS (MALDI–TOF) spectrum of compound **11**.

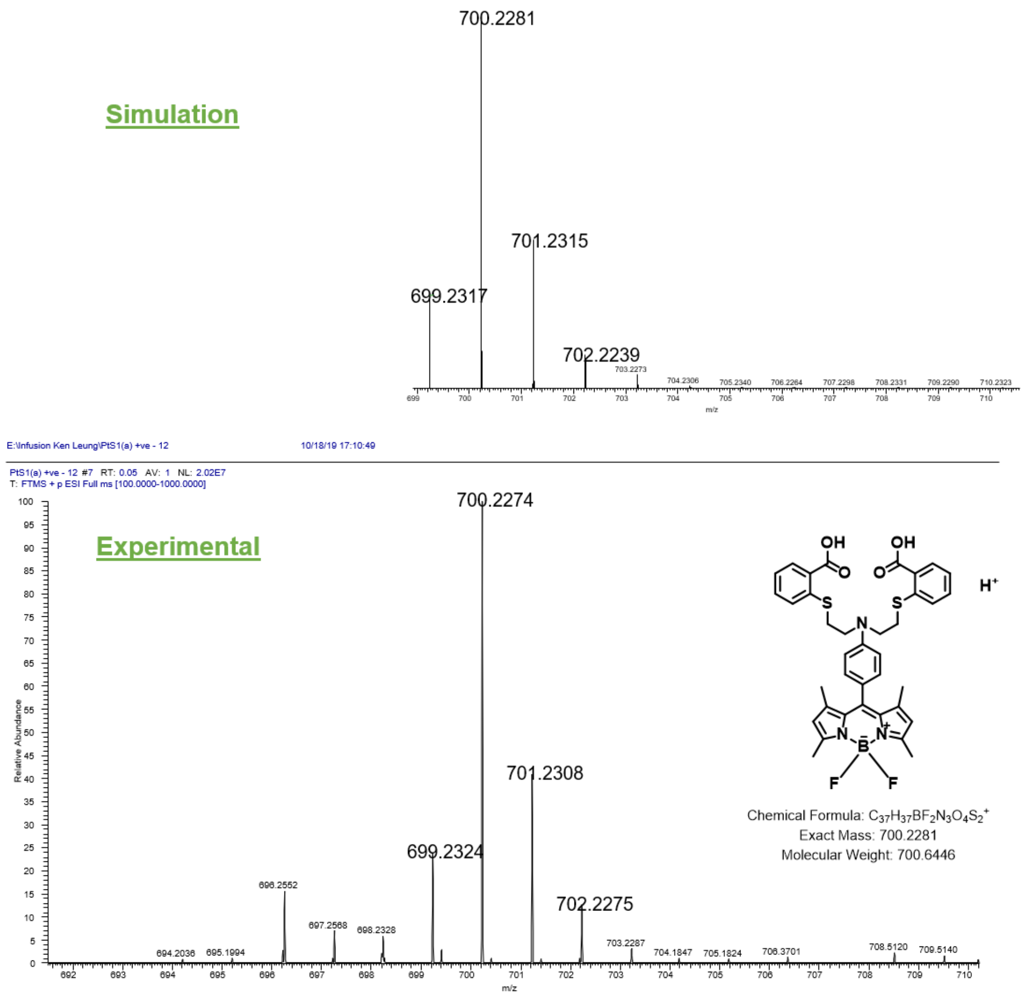

Figure S38. HRMS (+ESI) spectrum of **PS**.

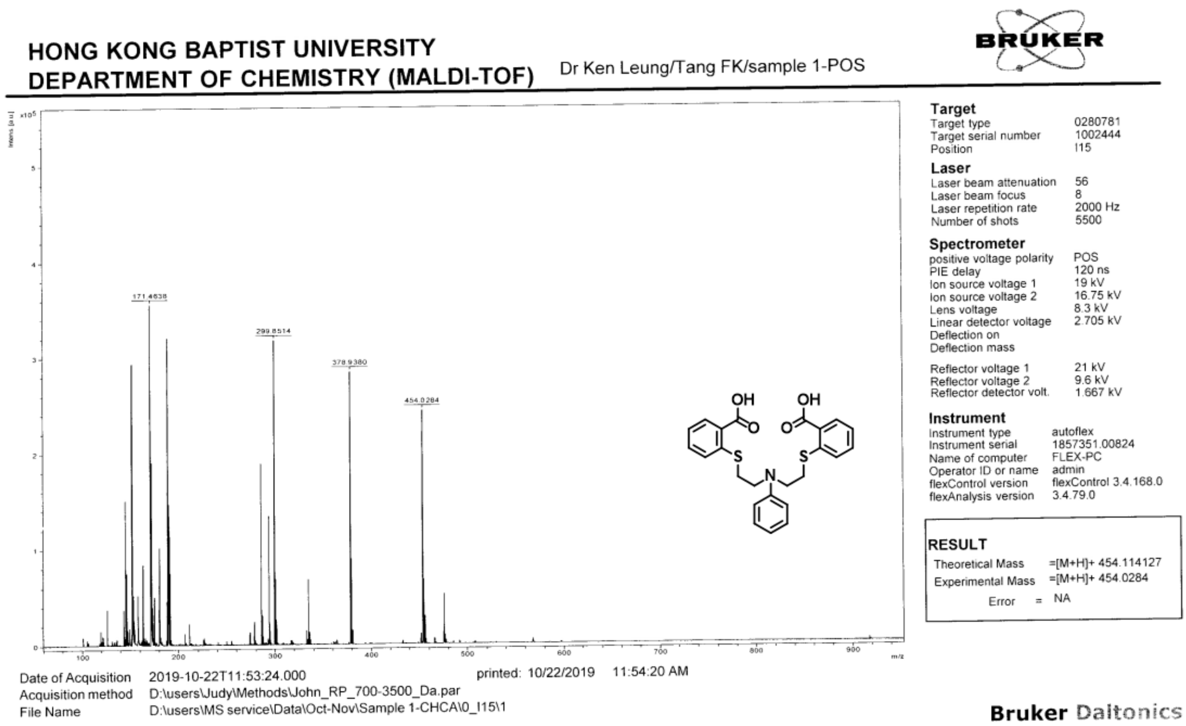

Figure S39. HRMS (MALDI–TOF) spectrum of compound **L**.

Table S2. Cartesian coordinates of the optimized ground-state geometry of **PS**.

1	N	5.919229	1.239149	0.109586	54	H	-1.029899	-2.618979	-0.547304
2	C	4.539673	1.218146	-0.084499	55	S	-2.921690	2.332338	0.910475
3	C	6.325736	2.519518	0.167409	56	S	-2.920923	-2.332706	0.910410
4	C	4.081958	2.570424	-0.148756	57	C	-3.817837	3.869798	1.040974
5	C	5.212140	3.362144	0.010466	58	C	-3.706136	4.543658	2.264089
6	H	5.243291	4.443962	0.014920	59	C	-4.636868	4.390946	0.023267
7	N	5.919323	-1.238757	0.109415	60	C	-4.412421	5.718827	2.501410
8	C	6.325900	-2.519105	0.167201	61	H	-3.048770	4.141123	3.030439
9	C	4.539759	-1.217825	-0.084610	62	C	-5.288224	5.606236	0.264354
10	C	5.212342	-3.361788	0.010295	63	C	-5.204684	6.258517	1.490537
11	C	4.082115	-2.570127	-0.148889	64	H	-4.321704	6.220237	3.460942
12	H	5.243558	-4.443605	0.014697	65	H	-5.885494	6.031424	-0.538347
13	B	6.833550	0.000221	0.242365	66	H	-5.744490	7.187693	1.652388
14	F	7.796259	0.000351	-0.769874	67	C	-3.816967	-3.870223	1.040873
15	F	7.467296	0.000137	1.487255	68	C	-4.636246	-4.391228	0.023301
16	C	7.747338	2.903880	0.369525	69	C	-3.704834	-4.544343	2.263809
17	H	8.124794	2.498472	1.313241	70	C	-5.287401	-5.606647	0.264309
18	H	8.374538	2.491270	-0.426468	71	C	-4.410938	-5.719626	2.501081
19	H	7.850803	3.989753	0.380207	72	H	-3.047265	-4.141922	3.030045
20	C	7.747517	-2.903388	0.369361	73	C	-5.203440	-6.259187	1.490320
21	H	8.374912	-2.489639	-0.425875	74	H	-5.884812	-6.031700	-0.538352
22	H	8.124529	-2.499073	1.313732	75	H	-4.319886	-6.221239	3.460476
23	H	7.851225	-3.989250	0.378782	76	H	-5.743096	-7.188455	1.652135
24	C	2.697077	-3.091338	-0.343651	77	C	-4.879604	3.722089	-1.334325
25	H	2.020550	-2.757643	0.449212	78	O	-4.603662	4.426796	-2.334845
26	H	2.262939	-2.752912	-1.289369	79	O	-5.352337	2.562436	-1.307998
27	H	2.710746	-4.183877	-0.344654	80	C	-4.879553	-3.722126	-1.334075
28	C	2.696906	3.091574	-0.343582	81	O	-4.604620	-4.426897	-2.334825
29	H	2.262964	2.753377	-1.289477	82	O	-5.351752	-2.562261	-1.307358
30	H	2.020265	2.757600	0.449062	83	N	-1.827084	0.000028	-0.923739
31	H	2.710486	4.184114	-0.344290					
32	C	3.855461	0.000139	-0.180562					
33	C	2.382445	0.000100	-0.384119					
34	C	1.519067	0.000067	0.713002					
35	C	1.846599	0.000096	-1.675635					
36	C	0.140007	0.000041	0.519835					
37	H	1.927134	0.000068	1.719768					
38	C	0.468884	0.000069	-1.864290					
39	H	2.512853	0.000114	-2.533851					
40	C	-0.400296	0.000043	-0.766820					
41	H	-0.537573	0.000018	1.368436					
42	H	0.067744	0.000069	-2.874269					
43	C	-2.332602	-1.214103	-1.562199					
44	H	-3.411608	-1.104131	-1.705588					
45	H	-1.878792	-1.381844	-2.556736					
46	C	-2.332599	1.214206	-1.562112					
47	H	-3.411559	1.104121	-1.705753					
48	H	-1.878622	1.382138	-2.556541					
49	C	-2.098313	2.453600	-0.719339					
50	H	-1.030216	2.618916	-0.546609					
51	H	-2.496202	3.326393	-1.241643					
52	C	-2.098047	-2.453625	-0.719683					
53	H	-2.496067	-3.326341	-1.242021					

Table S3. Cartesian coordinates of the optimized ground-state geometry of **PS+Pt^{2+}** in the O^S^S^O binding mode.

1	N	7.068638	1.255464	0.277305
2	C	5.703374	1.239011	0.000578
3	C	7.461961	2.532662	0.424449
4	C	5.240506	2.591090	-0.021288
5	C	6.353303	3.377872	0.245992
6	H	6.376585	4.458106	0.307811
7	N	7.090760	-1.218322	0.130953
8	C	7.504491	-2.497600	0.136961
9	C	5.724062	-1.193520	-0.138298
10	C	6.408015	-3.335868	-0.127948
11	C	5.281675	-2.542606	-0.303677
12	H	6.447968	-4.415998	-0.182676
13	B	7.986266	0.016040	0.383787
14	F	8.997961	0.082599	-0.576778
15	F	8.556059	-0.054290	1.656854
16	C	8.867354	2.911646	0.725003
17	H	9.198719	2.449977	1.660046
18	H	9.538347	2.552574	-0.061269
19	H	8.960796	3.995279	0.807813
20	C	8.916657	-2.885468	0.391003
21	H	9.580671	-2.424047	-0.346207
22	H	9.241359	-2.533546	1.374890
23	H	9.028433	-3.969540	0.344160
24	C	3.913613	-3.059961	-0.601441
25	H	3.186951	-2.754131	0.157390
26	H	3.538587	-2.693349	-1.561932
27	H	3.932146	-4.151815	-0.637020
28	C	3.865963	3.115838	-0.272624
29	H	3.482723	2.806614	-1.249772
30	H	3.149953	2.758179	0.473757
31	H	3.876369	4.207861	-0.239085
32	C	5.037280	0.024879	-0.204664
33	C	3.582063	0.028640	-0.511462
34	C	2.637761	-0.008485	0.515354
35	C	3.148764	0.065878	-1.840825
36	C	1.276498	-0.010814	0.217652
37	H	2.966556	-0.036317	1.550087
38	C	1.791216	0.062004	-2.135959
39	H	3.879186	0.094613	-2.644231
40	C	0.843234	0.022423	-1.107164
41	H	0.538567	-0.039375	1.014075
42	H	1.465706	0.085879	-3.172694
43	C	-1.035294	-1.249109	-1.983980
44	H	-1.959813	-1.043517	-2.528333
45	H	-0.319202	-1.674225	-2.703291
46	C	-1.072153	1.220141	-2.025474
47	H	-1.989683	0.968358	-2.562266
48	H	-0.370756	1.644656	-2.759296
49	C	-1.392126	2.308069	-1.010106
50	H	-0.489666	2.763383	-0.592541
51	H	-2.009767	3.088916	-1.459788
52	C	-1.322879	-2.310628	-0.931505
53	H	-1.925728	-3.120039	-1.349593
54	H	-0.407867	-2.731095	-0.504691
55	S	-2.280527	1.603483	0.442445
56	S	-2.215715	-1.570447	0.498903
57	C	-3.319235	2.963526	0.949079
58	C	-2.812505	3.731411	1.999708
59	C	-4.561565	3.262254	0.366245
60	C	-3.537374	4.811856	2.491345
61	H	-1.849713	3.475916	2.431870
62	C	-5.262719	4.362387	0.872993
63	C	-4.769459	5.124174	1.925567
64	H	-3.139508	5.400163	3.312096
65	H	-6.213169	4.604844	0.410545
66	H	-5.347364	5.962785	2.301390
67	C	-3.206339	-2.935334	1.083131
68	C	-4.441076	-3.304152	0.525219
69	C	-2.672245	-3.626699	2.172398
70	C	-5.107250	-4.393699	1.097340
71	C	-3.362346	-4.698651	2.728622
72	H	-1.716184	-3.317946	2.584207
73	C	-4.587006	-5.078979	2.188964
74	H	-6.051909	-4.690260	0.654835
75	H	-2.943520	-5.226961	3.579241
76	H	-5.137949	-5.911376	2.615660
77	C	-5.233083	2.544860	-0.787818
78	O	-6.039790	3.181486	-1.459726
79	O	-5.002652	1.289739	-1.035976
80	C	-5.132593	-2.675063	-0.667387
81	O	-5.924062	-3.370940	-1.297363
82	O	-4.927924	-1.433927	-0.995752
83	Pt	-3.678252	-0.026003	-0.266920
84	N	-0.562207	0.003623	-1.395682

Table S4. Cartesian coordinates of the optimized ground-state geometry of **PS+Pt^{2+}** in the O^S^N^O binding mode.

1	N	-6.484525	-1.411549	0.253778	54	C	3.906375	-3.173497	-0.140925
2	C	-5.116308	-1.391844	-0.006939	55	C	4.209192	-4.081144	-1.152623
3	C	-6.894558	-2.690949	0.301488	56	C	4.913117	-2.658124	0.696686
4	C	-4.669142	-2.744828	-0.124331	57	C	5.532452	-4.443604	-1.388862
5	C	-5.794058	-3.534661	0.071504	58	H	3.426821	-4.517871	-1.762900
6	H	-5.830790	-4.616083	0.052905	59	C	6.228139	-3.066504	0.453567
7	N	-6.471927	1.065927	0.312804	60	C	6.546240	-3.929222	-0.588254
8	C	-6.869564	2.345553	0.420234	61	H	5.759983	-5.135436	-2.193635
9	C	-5.104320	1.045234	0.048740	62	H	6.999351	-2.683862	1.113403
10	C	-5.761407	3.188548	0.226955	63	H	7.579792	-4.210111	-0.763502
11	C	-4.644599	2.397895	-0.007561	64	C	2.865036	4.378490	-0.561101
12	H	-5.787815	4.269981	0.258054	65	C	3.647778	3.583652	0.293081
13	B	-7.386962	-0.172261	0.453956	66	C	2.846709	5.765405	-0.376784
14	F	-8.388560	-0.143508	-0.518551	67	C	4.374418	4.187726	1.320382
15	F	-7.968386	-0.199662	1.722831	68	C	3.595681	6.359017	0.634687
16	C	-8.306586	-3.074065	0.562388	69	H	2.233448	6.378075	-1.031134
17	H	-8.634632	-2.693623	1.534519	70	C	4.357616	5.568909	1.490579
18	H	-8.969062	-2.635668	-0.190039	71	H	4.968966	3.565489	1.983985
19	H	-8.416114	-4.159225	0.547532	72	H	3.568602	7.437209	0.760308
20	C	-8.277491	2.729521	0.701117	73	H	4.935160	6.023109	2.289868
21	H	-8.944641	2.334359	-0.070882	74	C	4.731479	-1.751653	1.903787
22	H	-8.608600	2.305670	1.654048	75	O	5.550478	-1.838173	2.810470
23	H	-8.376349	3.815146	0.738742	76	O	3.741806	-0.902338	1.972808
24	C	-3.270095	2.920795	-0.262719	77	C	3.728626	2.090505	0.115853
25	H	-2.550893	2.562995	0.480383	78	O	4.583761	1.584391	-0.605192
26	H	-2.892854	2.614165	-1.243301	79	O	2.800643	1.466522	0.773158
27	H	-3.279212	4.012703	-0.228990	80	Pt	2.485779	-0.521293	0.459476
28	C	-3.298550	-3.269572	-0.397187	81	N	1.219385	-0.217645	-1.210775
29	H	-2.906817	-2.913613	-1.355061	82	C	1.032485	2.315304	-1.390386
30	H	-2.582854	-2.962819	0.372004	83	H	1.047656	2.315507	-0.300777
31	H	-3.321108	-4.361494	-0.423925	84	H	0.002200	2.461815	-1.721239
32	C	-4.434307	-0.173543	-0.108831					
33	C	-2.973781	-0.176832	-0.390370					
34	C	-2.050789	-0.207829	0.654363					
35	C	-2.508088	-0.151185	-1.707806					
36	C	-0.683560	-0.221043	0.388983					
37	H	-2.396798	-0.222926	1.683238					
38	C	-1.144861	-0.165266	-1.976589					
39	H	-3.215451	-0.119974	-2.530721					
40	C	-0.227319	-0.207851	-0.924406					
41	H	0.035286	-0.244122	1.203402					
42	H	-0.816082	-0.135311	-3.010641					
43	C	1.612980	1.026933	-1.968414					
44	H	2.703892	1.048812	-1.963292					
45	H	1.284705	0.913580	-3.008369					
46	C	1.562711	-1.387098	-2.097065					
47	H	2.614032	-1.275302	-2.373979					
48	H	0.963323	-1.350332	-3.012788					
49	C	1.329068	-2.705038	-1.396952					
50	H	0.276879	-2.849688	-1.136170					
51	H	1.631528	-3.547248	-2.019788					
52	S	2.193643	-2.745455	0.212648					
53	S	1.966150	3.774057	-1.979960					

Table S5. Cartesian coordinates of the optimized ground-state geometry of **PS+Pt^{2+}** in the O^S^N^S binding mode.

1	N	-6.484525	-1.411549	0.253778	54	H	3.906375	-3.173497	-0.140925
2	C	-5.116308	-1.391844	-0.006939	55	S	4.209192	-4.081144	-1.152623
3	C	-6.894558	-2.690949	0.301488	56	S	4.913117	-2.658124	0.696686
4	C	-4.669142	-2.744828	-0.124331	57	C	5.532452	-4.443604	-1.388862
5	C	-5.794058	-3.534661	0.071504	58	C	3.426821	-4.517871	-1.762900
6	H	-5.830790	-4.616083	0.052905	59	C	6.228139	-3.066504	0.453567
7	N	-6.471927	1.065927	0.312804	60	C	6.546240	-3.929222	-0.588254
8	C	-6.869564	2.345553	0.420234	61	H	5.759983	-5.135436	-2.193635
9	C	-5.104320	1.045234	0.048740	62	C	6.999351	-2.683862	1.113403
10	C	-5.761407	3.188548	0.226955	63	C	7.579792	-4.210111	-0.763502
11	C	-4.644599	2.397895	-0.007561	64	H	2.865036	4.378490	-0.561101
12	H	-5.787815	4.269981	0.258054	65	H	3.647778	3.583652	0.293081
13	B	-7.386962	-0.172261	0.453956	66	H	2.846709	5.765405	-0.376784
14	F	-8.388560	-0.143508	-0.518551	67	C	4.374418	4.187726	1.320382
15	F	-7.968386	-0.199662	1.722831	68	C	3.595681	6.359017	0.634687
16	C	-8.306586	-3.074065	0.562388	69	C	2.233448	6.378075	-1.031134
17	H	-8.634632	-2.693623	1.534519	70	C	4.357616	5.568909	1.490579
18	H	-8.969062	-2.635668	-0.190039	71	C	4.968966	3.565489	1.983985
19	H	-8.416114	-4.159225	0.547532	72	H	3.568602	7.437209	0.760308
20	C	-8.277491	2.729521	0.701117	73	C	4.935160	6.023109	2.289868
21	H	-8.944641	2.334359	-0.070882	74	H	4.731479	-1.751653	1.903787
22	H	-8.608600	2.305670	1.654048	75	H	5.550478	-1.838173	2.810470
23	H	-8.376349	3.815146	0.738742	76	H	3.741806	-0.902338	1.972808
24	C	-3.270095	2.920795	-0.262719	77	C	3.728626	2.090505	0.115853
25	H	-2.550893	2.562995	0.480383	78	O	4.583761	1.584391	-0.605192
26	H	-2.892854	2.614165	-1.243301	79	O	2.800643	1.466522	0.773158
27	H	-3.279212	4.012703	-0.228990	80	C	2.485779	-0.521293	0.459476
28	C	-3.298550	-3.269572	-0.397187	81	O	1.219385	-0.217645	-1.210775
29	H	-2.906817	-2.913613	-1.355061	82	O	1.032485	2.315304	-1.390386
30	H	-2.582854	-2.962819	0.372004	83	Pt	1.047656	2.315507	-0.300777
31	H	-3.321108	-4.361494	-0.423925	84	N	0.002200	2.461815	-1.721239
32	C	-4.434307	-0.173543	-0.108831					
33	C	-2.973781	-0.176832	-0.390370					
34	C	-2.050789	-0.207829	0.654363					
35	C	-2.508088	-0.151185	-1.707806					
36	C	-0.683560	-0.221043	0.388983					
37	H	-2.396798	-0.222926	1.683238					
38	C	-1.144861	-0.165266	-1.976589					
39	H	-3.215451	-0.119974	-2.530721					
40	C	-0.227319	-0.207851	-0.924406					
41	H	0.035286	-0.244122	1.203402					
42	H	-0.816082	-0.135311	-3.010641					
43	C	1.612980	1.026933	-1.968414					
44	H	2.703892	1.048812	-1.963292					
45	H	1.284705	0.913580	-3.008369					
46	C	1.562711	-1.387098	-2.097065					
47	H	2.614032	-1.275302	-2.373979					
48	H	0.963323	-1.350332	-3.012788					
49	C	1.329068	-2.705038	-1.396952					
50	H	0.276879	-2.849688	-1.136170					
51	H	1.631528	-3.547248	-2.019788					
52	C	2.193643	-2.745455	0.212648					
53	H	1.966150	3.774057	-1.979960					

References

1. M. J. Frisch, G. W. Trucks, H. B. Schlegel, G. E. Scuseria, M. A. Robb, J. R. Cheeseman, G. Scalmani, V. Barone, B. Mennucci, G. A. Petersson, H. Nakatsuji, M. Caricato, X. Li, H. P. Hratchian, A. F. Izmaylov, J. Bloino, G. Zheng, J. L. Sonnenberg, M. Hada, M. Ehara, K. Toyota, R. Fukuda, J. Hasegawa, M. Ishida, T. Nakajima, Y. Honda, O. Kitao, H. Nakai, T. Vreven, J. Montgomery, J. A., J. E. Peralta, F. Ogliaro, M. Bearpark, J. J. Heyd, E. Brothers, K. N. Kudin, V. N. Staroverov, T. Keith, R. Kobayashi, J. Normand, K. Raghavachari, A. Rendell, J. C. Burant, S. S. Iyengar, J. Tomasi, M. Cossi, N. Rega, J. M. Millam, M. Klene, J. E. Knox, J. B. Cross, V. Bakken, C. Adamo, J. Jaramillo, R. Gomperts, R. E. Stratmann, O. Yazyev, A. J. Austin, R. Cammi, C. Pomelli, J. W. Ochterski, R. L. Martin, K. Morokuma, V. G. Zakrzewski, G. A. Voth, P. Salvador, J. J. Dannenberg, S. Dapprich, A. D. Daniels, O. Farkas, J. B. Foresman, J. V. Ortiz, J. Cioslowski and D. J. Fox, Gaussian, Inc., Wallingford CT, 2016.

2. J. P. Perdew, K. Burke and M. Ernzerhof, *Phys. Rev. Lett.*, 1996, **77**, 3865-3868.

3. J. P. Perdew, K. Burke and M. Ernzerhof, *Phys. Rev. Lett.*, 1997, **78**, 1396-1396.

4. C. Adamo and V. Barone, *J. Chem. Phys.*, 1999, **110**, 6158-6170.

5. V. Barone and M. Cossi, *J. Phys. Chem. A*, 1998, **102**, 1995-2001.

6. M. Cossi, N. Rega, G. Scalmani and V. Barone, *J. Comput. Chem.*, 2003, **24**, 669-681.

7. D. Andrae, U. Haussermann, M. Dolg, H. Stoll and H. Preuss, *Theor. Chim. Acta.*, 1990, **77**, 123-141.

8. A. W. Ehlers, M. Böhme, S. Dapprich, A. Gobbi, A. Höllwarth, V. Jonas, K. F. Köhler, R. Stegmann, A. Veldkamp and G. Frenking, *Chem. Phys. Lett.*, 1993, **208**, 111-114.

9. W. J. Hehre, Ditchfie.R and J. A. Pople, *J. Chem. Phys.*, 1972, **56**, 2257-2261.

10. P. C. Hariharan and J. A. Pople, *Theor. Chim. Acta.*, 1973, **28**, 213-222.

11. M. M. Francl, W. J. Pietro, W. J. Hehre, J. S. Binkley, M. S. Gordon, D. J. Defrees and J. A. Pople, *J. Chem. Phys.*, 1982, **77**, 3654-3665.

12. X. Zheng, C. Liang, L. Wang, B. Wang, Y. Liu, S. Feng, J. Z. Wu, L. Gao, L. Feng, L. Chen, T. Guo, H. C. Shen and H. Yun, *J. Med. Chem.*, 2018, **61**, 10228-10241.

13. M. K. Pola, M. V. Ramakrishnam Raju, C.-M. Lin, R. Putikam, M.-C. Lin, C. P. Epperla, H.-C. Chang, S.-Y. Chen and H.-C. Lin, *Dyes Pigm.*, 2016, **130**, 256-265.

14. Q. Dong, M. J. Rose, W.-Y. Wong and H. B. Gray, *Inorg. Chem.*, 2011, **50**, 10213-10224.

15. A. L. Garner and K. Koide, *Chem. Commun.*, 2009, 83-85.

16. L. Zhou, Y. Feng, J. Cheng, N. Sun, X. Zhou and H. Xiang, *RSC Adv.*, 2012, **2**, 10529-10536.

17. H. Kim, S. Lee, J. Lee and J. Tae, *Org. Lett.*, 2010, **12**, 5342-5345.

18. C. Shen, B. D. W. Harris, L. J. Dawson, K. A. Charles, T. W. Hambley and E. J. New, *Chem. Commun.*, 2015, **51**, 6312-6314.

19. D. Montagner, S. Q. Yap and W. H. Ang, *Angew. Chem. Int. Ed.*, 2013, **52**, 11785-11789.

20. J. X. Ong, C. S. Q. Lim, H. V. Le and W. H. Ang, *Angew. Chem. Int. Ed.*, 2019, **58**, 164-167.